N-benzylpiperidinol derivatives as novel USP7 inhibitors: Structure–activity relationships and X-ray crystallographic studies

Minglei Li, Shengjie Liu, Hui Chen, Xinyu Zhou, Jin Zhou, Shuxi Zhou, Haoliang Yuan, Qing-Long Xu, Jun Liu, Keguang Cheng, Hongbin Sun, Yue Wang, Caiping Chen, Xiaoan Wen

PII: S0223-5234(20)30248-8

DOI: https://doi.org/10.1016/j.ejmech.2020.112279

Reference: EJMECH 112279

To appear in: *European Journal of Medicinal Chemistry*

Received Date: 25 January 2020

Revised Date: 25 March 2020

Accepted Date: 25 March 2020

Please cite this article as: M. Li, S. Liu, H. Chen, X. Zhou, J. Zhou, S. Zhou, H. Yuan, Q.-L. Xu, J. Liu, K. Cheng, H. Sun, Y. Wang, C. Chen, X. Wen, N-benzylpiperidinol derivatives as novel USP7 inhibitors: Structure–activity relationships and X-ray crystallographic studies, *European Journal of Medicinal Chemistry* (2020), doi: https://doi.org/10.1016/j.ejmech.2020.112279.

N-benzylpiperidinol derivatives as novel USP7 inhibitors: structure–activity relationships and X-ray crystallographic studies

Minglei Li [a,†], Shengjie Liu [a,†], Hui Chen [a,†], Xinyu Zhou [a], Jin Zhou [a], Shuxi Zhou [a], Haoliang Yuan [a], Qing-Long Xu [a], Jun Liu [a], Keguang Cheng [b], Hongbin Sun [a], Yue Wang [c,*], Caiping Chen [a,*], Xiaoan Wen [a,*]

[a] *Jiangsu Key Laboratory of Drug Discovery for Metabolic Disease, State Key Laboratory of Natural Medicines, China Pharmaceutical University, Nanjing 210009, China*

[b] *State Key Laboratory for the Chemistry and Molecular Engineering of Medicinal Resources, School of Chemistry and Pharmacy of Guangxi Normal University, Guilin 541004, China*

[c] *School of Science, China Pharmaceutical University, Nanjing 211198, China*

[†] These authors contributed equally to this article.

[*] Corresponding authors: Tel/fax: +86-25-83271050. E-mail: *wxagj@126.com* (X. A. Wen); caiping.chen@cpu.edu.cn (C. P. Chen); zwy_1115@126.com (Y. Wang)

Graphical abstract

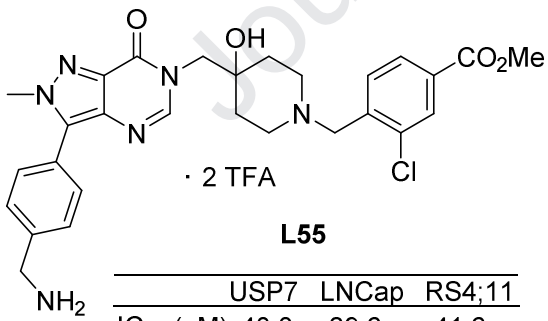

L55

	USP7	LNCap	RS4;11
IC_{50} (nM)	40.8	29.6	41.6
K_D (nM)	78.3		

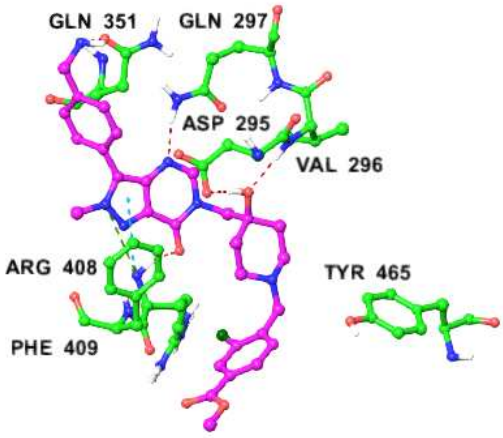

Highlights

- *Fifty-five piperidinol derivatives were synthesized and biologically evaluated.*
- *Compound* **L55** *exhibited potent USP7 inhibitory activity (IC_{50} = 40.8 nM).*

- *X-ray crystallographic studies revealed a new pose for* **L55** *to bind to USP7.*
- **L55** *downregulated MDM2 and DNMT1 and upregulated p53 and p21 in RS4;11 cells.*
- *LNCaP (IC_{50} = 29.6 nM) and RS4;11 (IC_{50} = 41.6 nM) were highly sensitive to* **L55**.

Abstract

USP7 as a deubiquitinase plays important roles in regulating the stability of some oncoproteins including MDM2 and DNMT1, and thus represents a potential anticancer target. Through comparative analysis of USP7 co-crystal structures in complex with the reported piperidinol inhibitors, we noticed that the USP7 Phe409 sub-site might have good adaptability to the ligands. Based on this observation, 55 N-aromatic and N-benzyl piperidinol derivatives were designed, synthesized and biologically evaluated, among which compound **L55** was identified as a highly selective and potent USP7 inhibitor (IC_{50} = 40.8 nM, K_D = 78.3 nM). X-ray crystallographic studies revealed that **L55** bound to USP7 with a new pose that was very different from the previously reported inhibitors. The results of cellular assays showed that **L55** had strong antitumor activity against LNCaP (IC_{50} = 29.6 nM) and RS4;11 (IC_{50} = 41.6 nM) cells, probably through inducing cell death and restricting G0/G1 and S phases. Moreover, **L55** dose-dependently reduced the protein levels of MDM2 and DNMT1 and increased the protein levels of p53 and p21. These findings could have valuable implications for designing novel structural classes of USP7 inhibitors.

Key words: USP7, piperidine, structure-activity relationship, crystallographic study, deubiquitinase

1. INTRODUCTION

The ubiquitin–proteasome system (UPS) is critical to maintain protein homeostasis

in the human body. With ubiquitin (a highly conserved 76-amino-acid polypeptide) linked to or removed from target proteins [1], the fates of these proteins can be regulated in many aspects, such as cellular localization, physiological functions and protein stability [2]. Not surprisingly, abnormal modulation of the UPS is closely correlated to various diseases (*e.g.*, cancer [3], infection [4], and neurodegeneration [5]). Therefore, pharmacological interference of UPS represents a promising therapeutic approach to diseases such as cancer, as evidenced by the approval of the proteasome inhibitor bortezomib for the treatment of multiple myeloma and mantle cell lymphoma [6]. As an important component of the UPS, deubiquitinating enzymes play a key role in maintaining the normal functions of the UPS [7-10]. Ubiquitin-specific proteases (USP) constitute the largest family of deubiquitinating enzymes, among which ubiquitin-specific protease 7 (USP7, also known as HAUSP) has been extensively investigated as a potential target for cancer treatment. Notably, USP7 deubiquitinates and stabilizes MDM2, leading to decreased stability of the tumor suppressor p53 [11, 12]. Inhibition of USP7 has been shown to increase p53 stability, thus promoting cancer cell apoptosis [12-14]. In addition, USP7 deubiquitinates many other proteins, including DNMT1 [15], N-Myc [16] and Tip60 [17, 18], among others. Thus, inhibition of USP7 can also induce anti-tumor effects in a p53-independent manner [19].

Early efforts by other research groups identified several classes of USP7 inhibitors, including **HBX41108**, **HBX19818** and **P5091** (Fig. 1) [20-22], but the potency and selectivity of theses inhibitors were poor. Recently, a series of piperidinol derivatives (Fig. 1: **FT671**, **FT827**, **CP4**, **CP5**) were identified as potent and highly selective USP7 inhibitors [23-26], and facile semi-synthetic methods were established to produce key probe reagents for exploring deubiquitinase activity [27, 28]. X-ray crystallographic studies revealed that the piperidinol and pyrimidone subunits in **FT671** and **CP5** were two key pharmacophores with important hydrogen bond interactions with USP7 Asp295, Val296, Gln297 and Phe409, respectively [24, 26]. In particular, we noticed that the Phe409 sub-site of USP7 showed a great adaption to the ligands, which could be used for the design of new inhibitors.

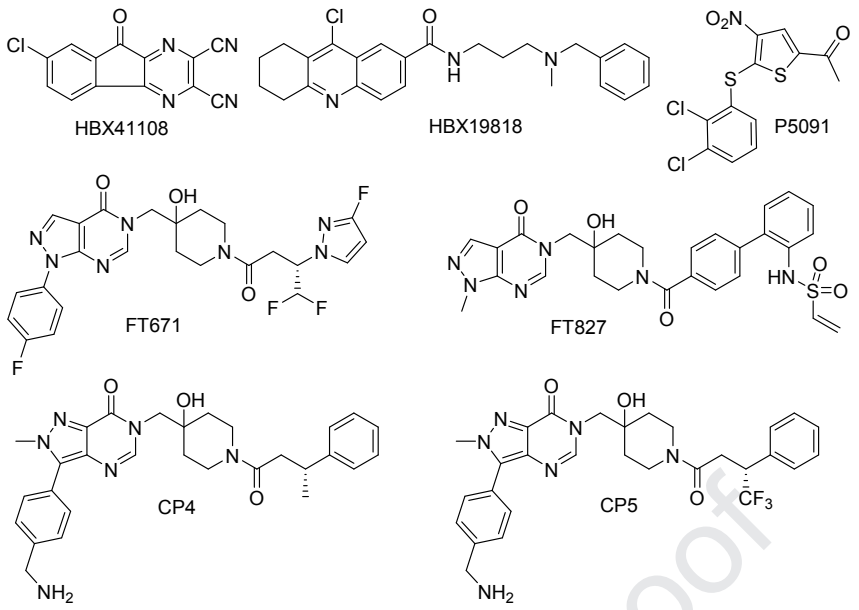

Fig. 1. Structures of some USP7 inhibitors.

As a part of our program to develop novel USP7 inhibitors for cancer therapy [16, 29, 30], we worked on the structural modifications of the piperidinol class of USP7 inhibitors, with a particular focus on the USP7 Phe409 sub-site. Thus, a series of N-aromatic and N-benzyl piperidinol derivatives were designed, synthesized and biologically evaluated. Among these compounds, compound **L55** was found to potently inhibit USP7 (IC_{50} = 40.8 nM, K_D = 78.3 nM). Moreover, **L55** showed strong antiproliferative activity in the cancer cell lines LNCaP (IC_{50} = 29.6 nM) and RS4;11 (IC_{50} = 41.6 nM). More importantly, X-ray crystallographic studies revealed that **L55** bound to USP7 with a new pose that was very different from the previously reported inhibitors.

2. RESULTS AND DISCUSSION

2.1 Design of target compounds

Considering that the USP7 Phe409 sub-site exhibited great adaptability to the ligands, we examined the potency outcome of replacing the flexible long chain of **FT671** with a heteroaromatic group, and thus, a series of N-heteroaromatic piperidinol derivatives (Fig. 2: **L1**-**L13**) were designed. It was expected that the

heteroatoms could make hydrogen bond interactions with USP7 Try 465, and the heteroaromatic rings could mimic the bending pose of the long chain of **FT671**.

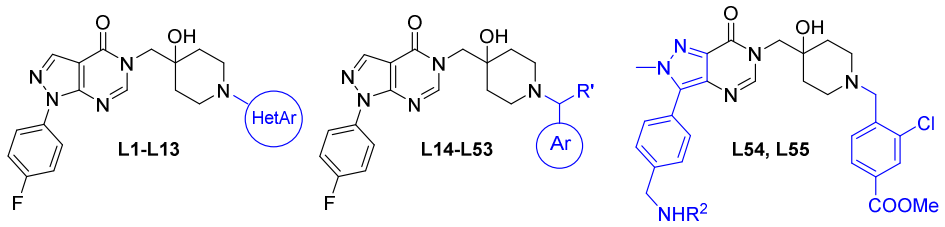

Fig. 2. Design of the target compounds.

In addition, we noticed that although the piperidinol amide group of **FT827** hydrogen bonded with USP7 Try465, it also formed a dihedral angle of nearly 90 degrees with its attached phenyl group [23]. Thus, we considered deleting the amide oxygen atom and the outer phenyl group of the diphenyl so that the ligands could be easily adjusted to the optimal binding poses. In this regard, a series of N-benzyl piperidinol derivatives were designed (Fig. 2: **L14-L53**). Furthermore, upon finding 2-chloro-4-methoxycarbonylbenzyl as one of the preferred groups, compounds **L54** and **L55** were designed, as the (4-aminomethyl)phenyl group and the pyrazolo[4,3-d]pyrimidine skeleton were reported to add more hydrogen bond interactions with USP7 [24].

2.2 Synthesis of target compounds

The synthetic route to **L1-L49** is depicted in Scheme 1. The key intermediate **5** was synthesized according to previously reported procedure [23]. In the presence of triethylamine, 4-fluorophenylhydrazine hydrochloride and 2-(ethoxymethylene)malonoitrile were cyclized under heating to form pyrozole **1**, which was hydrolyzed to afford amide **2**. Reaction of **1** with triethyl methanetricarboxylate in acetic anhydride under reflux afforded pyrimidone **3**, followed by a nucleophilic substitution reaction occurring with tert-butyl 1-oxa-6-azaspiro[2.5]octane-6-carboxylate in the presence of Cs_2CO_3 to give piperidinol **4**. Compound **4** was Boc-deprotected by TFA and finally reacted with diverse halides to offer the target compounds **L1-L49**. Ester **L49** was hydrolyzed in

50% hydroxylamine aqueous solution to give carboxylic acid **L50**, which was amidated with different amines to provide **L51-L53**.

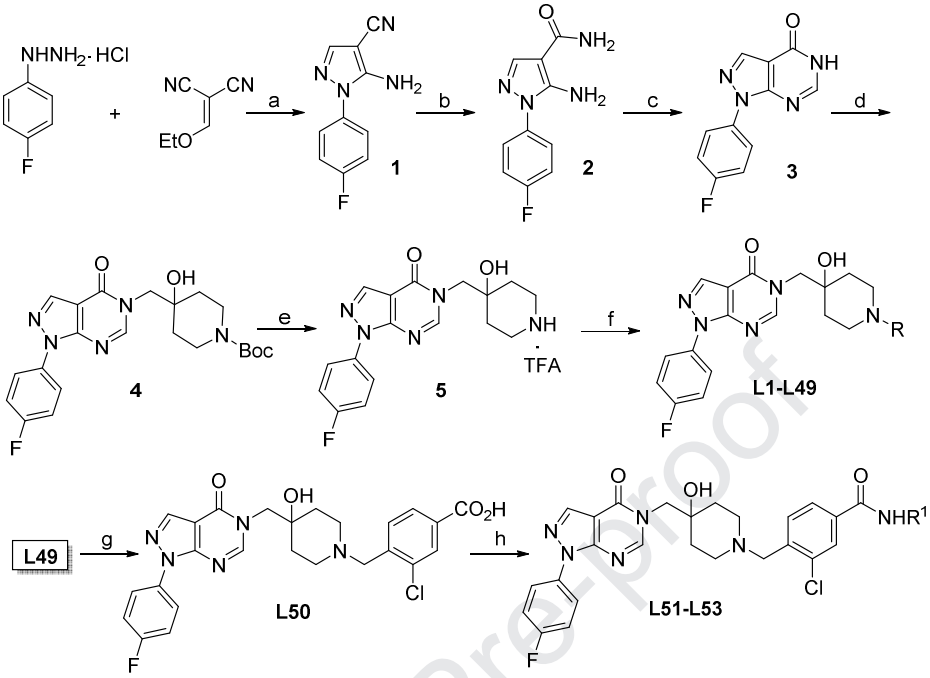

Scheme 1. Synthesis of **L1-L49**. Reagents and conditions: (a) TEA, EtOH, reflux, 10 h, 66%; (b) con. H_2SO_4, r.t., 75%; (c) triethyl orthoformate, acetic anhydride, reflux, 53%; (d) tert-butyl 1-oxa-6-azaspiro[2.5]octane-6-carb-oxylate, Cs_2CO_3, DMF, 80 ℃, 33%; (e) TFA, DCM, r.t.; (f) K_2CO_3, DMF, r.t. or 120 ℃, 16-86%; (g) 50% NH_2OH in H_2O, 90 ℃, 73%; (h) for **L51** or **L53**: oxalyl chloride, DMF (cat.), DCM; then ammonia methanol solution or 50% NH_2OH in H_2O, r.t., 30% or 31%; for **L52**: 27% methylamine in EtOH, HATU, DIPEA, DMF, r.t., 40%.

The synthesis of **L54** and **L55** is outlined in Scheme 2. The intermediate **11** was prepared from commercially available methyl 4-nitro-1H-pyrazole-3-carboxylate over six steps: methylation, reduction, cyclization, bromination, aminolysis cleavage of epoxy and Boc-deprotection [24]. Treatment of **11** with methyl 4-(bromomethyl)-3-chlorobenzoate in the presence of potassium carbonate gave compound **12**, which reacted with boronate **15** or **16** under Suzuki coupling conditions to afford **17** or **L54**. Boc-deprotection of **17** in trifluoroacetic acid gave compound **L55** as the trifluoroacetate form.

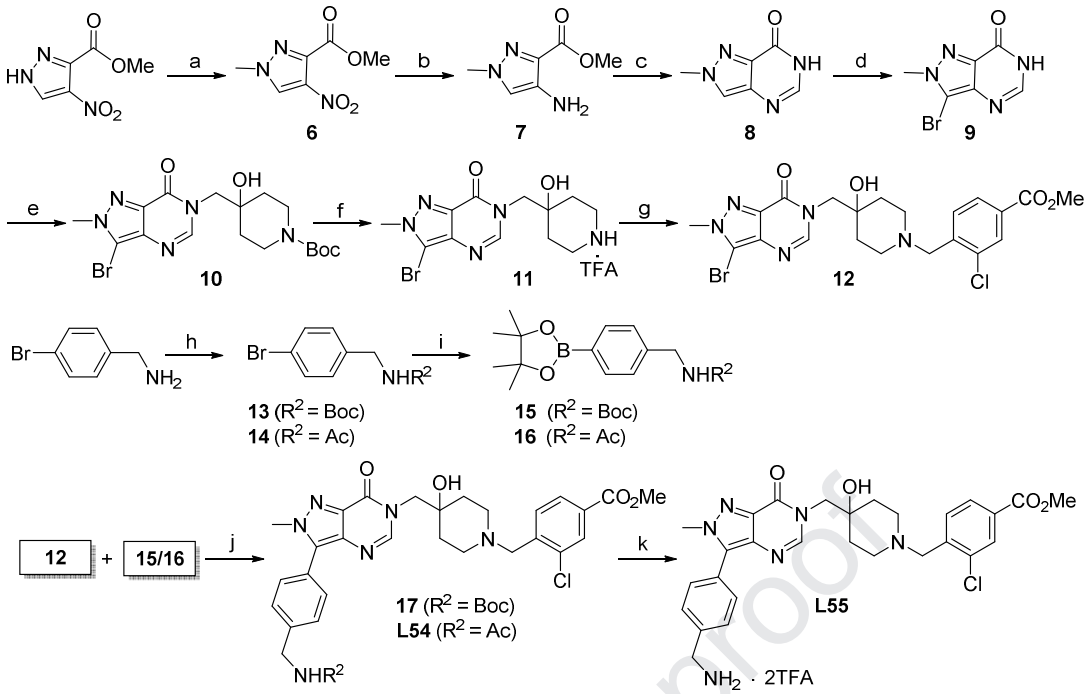

Scheme 2. Synthesis of **L54** and **L55**. Reagents and conditions: (a) K_2CO_3, MeI, acetone, 70 □, 27%; (b) Pd/C, H_2, MeOH, r.t., 97%; (c) formamidine acetate, DIPEA, *n*-BuOH, 110 °C, 94%; (d) Br_2, AcOH, 95 °C, 36%; (e) tert-butyl 1-oxa-6-azaspiro[2.5]octane-6-carboxylate, Cs_2CO_3, DMF, 80 °C, 33%; (f) TFA, DCM, r.t.; (g) methyl 4-(bromomethyl)-3-chlorobenzoate, K_2CO_3, DMF, r.t., 32%; (h) for **13**: $(Boc)_2O$, N_2, DIPEA, $CHCl_3$, r.t., 92%; for **14**: acetyl chloride, TEA, dry DCM, 76%; (i) AcOK, Bis(pinacolato)diboron, $Pd(dppf)Cl_2$, DMSO, Ar, 80 °C, 16-95%; (j) $Pd(PPh_3)_4$, K_2CO_3, DMF, Ar, 110 °C, 60-65%; (k) TFA, DCM, r.t., 79%.

2.3 USP7 inhibitory activity and SAR analysis of the target compounds

The inhibitory activity of all the target compounds against full-length USP7 was evaluated using a Ub-Rho assay [30] with the trifluoroacetic acid salt of **CP4** as the positive control (its synthetic details are included in Supporting Information). A preliminary screen was performed at a compound concentration of 10 μM or 1 μM. For those compounds with inhibition ≥50%, IC_{50} values were further determined.

As shown in Table 1, all N-aromatic compounds had poor or no activity at 10 μM, with the exception of halides **L5-L7**, which had 32-43% inhibition against USP7.

Table 1. USP7 inhibitory activity of **L1**-**L13**

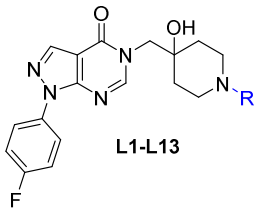

L1-L13

Cpd	R	Inhibition (%)	Cpd	R	Inhibition (%)
L1		NA	**L8**		NA
L2		NA	**L9**	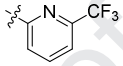	NA
L3	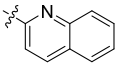	15.5±2.2	**L10**	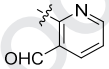	21.9±7.8
L4		19.6±4.4	**L11**	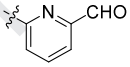	NA
L5		32.1±1.0	**L12**		NA
L6		43.3±5.2	**L13**	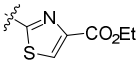	NA
L7		39.3±6.4	**CP4**	(trifluoroacetic acid salt)	92.4±6.8 [a]

[a] Determined at a compound concentration of 1 μM. NA: not active.

As shown in Table 2, N-benzyl piperidinol compound **L14** exhibited poor activity, and no improvement was observed on aza-benzyl compounds **L15-17**. Notably, introduction of NO_2, CN, halides and COOMe to the ortho (**L20**, **L23**, **L25**, **L28** and **L30**) and para (**L22**, **L24**, **L27**, **L29** and **L31**) positions of the phenyl group of the N-benzyl fragments generally led to a large increase in activity. In particular, ortho chloride **L25**, ortho bromide **L28** and para ester **L37** had IC_{50} values of 3.4, 3.1 and 4.5 μM, respectively. In contrast, ortho ester **L35** was not active, and compounds **L32-L34**, with electron-donating groups CH_3 and CF_3, had poor activity, indicating a strong preference of small and electron-withdrawn groups for the ortho and para positions.

The above findings prompted us to investigate ortho and para di-substituted compounds. To our delight, combinations of ortho-halides and para-COOMe

dramatically improved the activity. Compounds **L43** (IC_{50} = 0.8 μM), **L44** (IC_{50} = 0.8 μM) and **L45** (IC_{50} = 0.9 μM) bearing both ortho-halides and para-COOMe were more potent than compounds **L23** (IC_{50} = 9.8 μM), **L25** (IC_{50} = 3.4 μM) and **L28** (IC_{50} = 3.1 μM) bearing only ortho-halides. Notably, very small structural changes on methyl ester **L44** caused sharp decrease in potency since acid **L50** and amides **L51-53** were almost not active at 1 μM.

Table 2. USP7 inhibitory activity of **L14-L53**

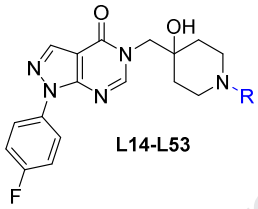

L14-L53

Cpd	R	Inhibition (%)	IC_{50} (μM)	Cpd	R	Inhibition (%)	IC_{50} (μM)
L14		24.9±7.1	ND	**L35**	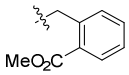	NA	ND
L15	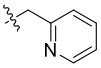	NA	ND	**L36**	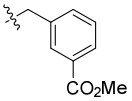	NA	ND
L16	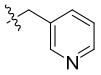	20.7±5.5	ND	**L37**	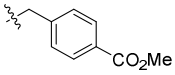	65.2±20.7	4.5±0.6
L17	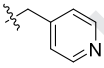	14.3±6.6	ND	**L38**	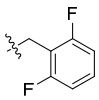	28.6±5.8	ND
L18	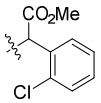	NA	ND	**L39**	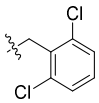	17.1±7.1	ND
L19	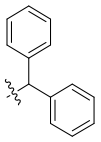	NA	ND	**L40**	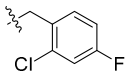	75.3±0.7	1.6±0.4
L20	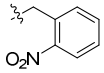	40.5±5.3	ND	**L41**	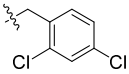	66.5±18.3	3.3±0.9
L21	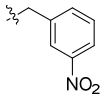	21.4±4.5	ND	**L42**	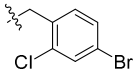	72.7±2.9	1.9±0.6
L22	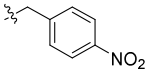	53.7±3.8	9.0±4.5	**L43**	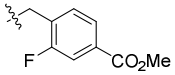	61.1±3.3 [a]	0.8±0.3

Cpd	R	Inhibition (%)	IC_{50} (μM)	Cpd	R	Inhibition (%)	IC_{50} (μM)
L23	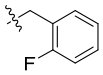	59.6±4.5	9.8±1.2	**L44**	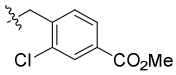	65.9±3.7 [a]	0.8±0.2
L24	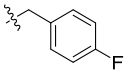	30.9±7.8	ND	**L45**	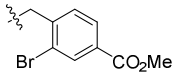	55.7±6.7 [a]	0.9±0.2
L25	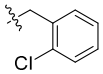	82.4±1.5	3.4±0.4	**L46**	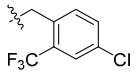	41.2±5.5	ND
L26	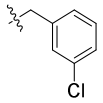	23.9±6.9	ND	**L47**	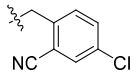	62.9±18.6	11.4±1.2
L27	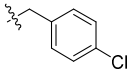	60.6±21.5	8.0±0.9	**L48**	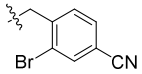	43.5±3.9	ND
L28	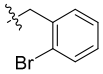	68.6±10.3	3.1±0.4	**L49**	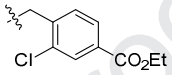	42.7±5.1 [a]	ND
L29	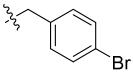	51.9±3.0	6.7±1.8	**L50**	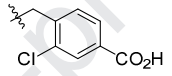	17.8±8.1 [a]	ND
L30	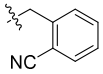	59.4±13.2	8.1±2.7	**L51**	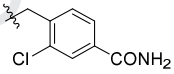	NA [a]	ND
L31	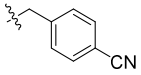	18.2±5.7	ND	**L52**	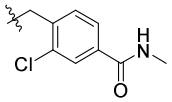	NA [a]	ND
L32	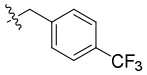	34.9±3.8	ND	**L53**	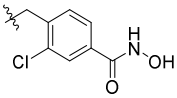	NA [a]	ND
L33	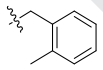	31.8±5.2	ND				
L34	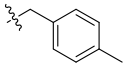	23.1±5.6	ND	**CP4**	(trifluoroacetic acid salt)	92.4±6.8 [a]	0.0197±0.0072

[a] Determined at a compound concentration 1 μM; NA: not active; ND: not determined.

As shown in Table 3, replacing the pyrazolo[3,4-d]pyrimidone fragment with the pyrazolo[4,3-d]pyrimidone fragment significantly increased the potency, consistent with a previous report [24]. The intermediate **12** (IC_{50} = 156.6 nM) was 4 times more potent than **L44**. Substitution of the bromine atom of **12** with 4-aminomethylphenyl group further improved the potency by approximately 4-fold, giving rise to the most potent compound in this study, **L55** (IC_{50} = 40.8 nM). Boc-protection or acetylation of the benzylamino group of **L55** caused a significant reduction of potency (compound **17** IC_{50} = 208.8 nM; **L54** IC_{50} = 121.3 nM).

Table 3. USP7 inhibitory activity of **12**, 17, **L54** and **L55**

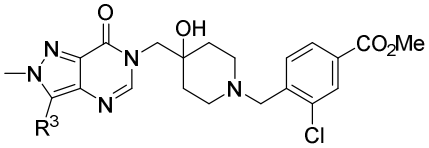

Cpd	R^3	IC_{50} (nM)
12	Br	156.6±9.5
17	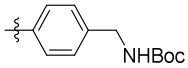	208.8±21.9
L54	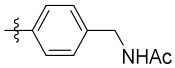	121.3±0.56
L55	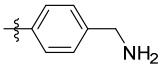 (trifluoroacetic acid salt)	40.8±4.4
CP4	(trifluoroacetic acid salt)	19.7±7.2

The deubiquitinase inhibitory selectivity of compound

L55 was further evaluated. As shown in Table S4 (see Supporting Information), similar to the control compound **CP4** (trifluoroacetic acid salt), compound **L55** did not inhibit a panel of the tested deubiquitinases UCH-L1, UCH-L5, USP2, USP25, USP28 and USP11 at 20 μM, indicating its excellent inhibitory selectivity for USP7.

2.4 Binding affinity of L55 to USP7

The binding affinity of **L55** to USP7 was determined using Biolayer Interferometry (BLI) technology. As shown in Fig. 3, **L55** bound to the USP7 catalytic domain with high affinity (K_D = 78.3 nM), which was comparable to the positive control **CP4** (trifluoroacetic acid salt, K_D = 41.6 nM) and consistent with the IC_{50} values.

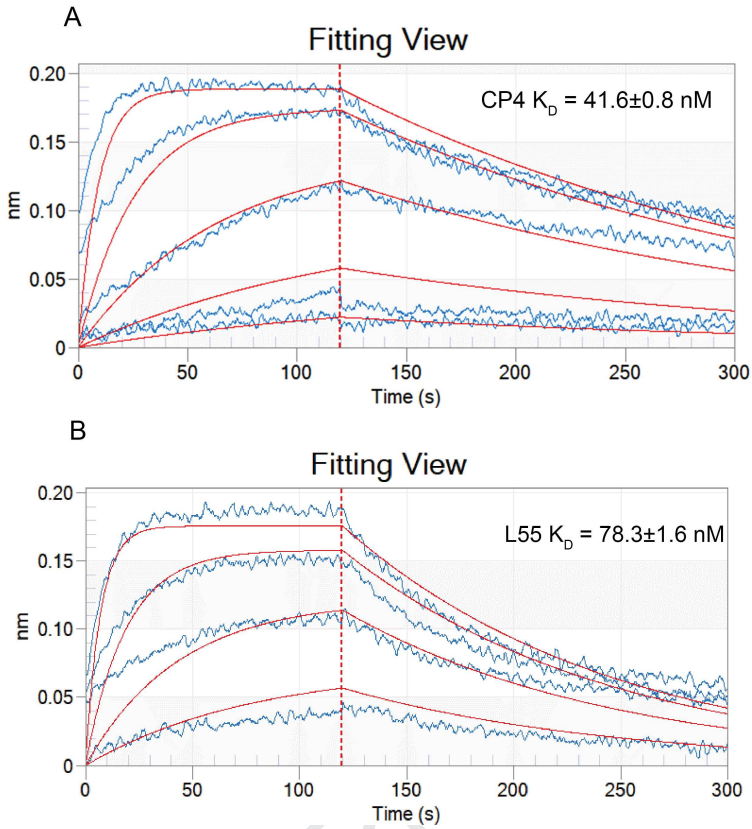

Fig. 3. Binding profiles for the interaction of **CP4** (A) and **L55** (B) with the USP7 catalytic domain (determined by BLI).

2.5 X-ray crystallographic study of USP7 co-crystals in complex with L55

To reveal the crucial interactions between compound **L55** and USP7, we cultivated co-crystals of USP7 catalytic domain protein with **L55** and determined their structure by an X-ray diffraction method. A co-crystal structure at 2.26 Å resolution was successfully obtained. The X-ray crystallographic studies showed that similar to **CP5** [24], **L55** bound to USP7 in the ubiquitin C-terminal binding cleft between the palm and thumb areas (Fig. 4A and Fig. 4B). The rigid skeletons of **L55** and **CP5** had very similar poses and interactions with USP7 (Fig. 4C and Fig. 4D). Their (4-aminomethyl)phenyl groups both stretched out to the USP7 surface and made hydrogen bond interactions with Gln351. Their pyrazolopyrimidone groups were both buried in USP7 and made multiple hydrogen bond interactions with Gln297, Arg408 and Phe409.

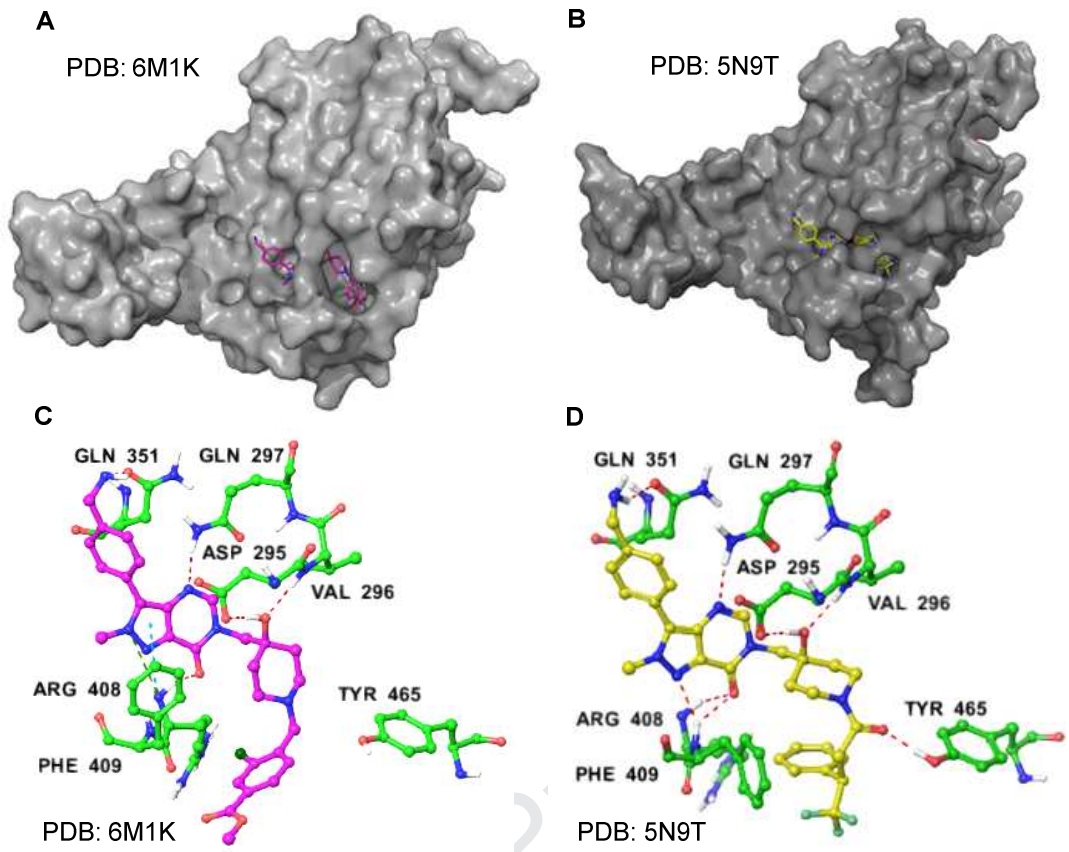

Fig. 4. Comparison of the co-crystal structures of **L55** (A, C) and **CP5** (B, D) binding to the USP7 catalytic domain.

Unexpectedly, in the USP7 complex with **L55**, Phe409 showed a large upshift, thus adding good pi-pi interactions to the pyrazole ring of **L55** (Fig. 4C). Moreover, **L55** was very different from **CP5** in the pose of the piperidinol group (Fig. 4D), although their hydroxyl groups both made hydrogen bond interactions with Asp295 and Val296. The piperidinol ring of **L55** stood up and was nearly parallel to the pyrimidone ring, probably due to the lack of a hydrogen bond interaction with Tyr465, while the piperidinol ring of **CP5** laid flat in the USP7 pocket. Additionally, unlike the flexible chain in **CP5**, the benzyl group of **L55** did not bend inward but stretched outside, which was probably the cause of the Phe409 shift. The 2-chloro and 4-methoxycarbonyl groups on the benzyl of **L55** were very close to the binding pocket boundary, thus not allowing for replacement by large groups. Together, this new co-crystal structure would assist in the design of novel USP7 inhibitors.

2.6 *In vitro* anticancer effect and action mechanism of L55

We next performed the cell viability assay for compound **L55** against a panel of cancer cell lines including LNCaP, RS4;11, HCT116, NB4, K562 and Huh-7 cells. RS4;11 (lymphoblastic leukemia cell line) and LNCaP (prostate cancer cell line) were previously reported to be highly sensitive to **CP4** [24]. As expected, we found that among the test cell lines, RS4;11 and LNCaP were the most sensitive to **L55** and **CP4**. As shown in Table 4, **L55** exhibited nanomolar levels of inhibitory activity on LNCaP and RS4;11 and was slightly less potent than **CP4**. Conversely, **L55** showed very weak inhibitory activity on HCT116, NB4, K562 and Huh-7 cells (see Supporting Information Fig. S3).

Table 4. Inhibitory activity of **L55** and **CP4** on cancer cell growth

Cpd	LNCaP IC_{50}/nM	RS4;11 IC_{50}/nM	HCT116 IC_{50}/μM	NB4 IC_{50}/μM	K562 IC_{50}/μM	Huh-7 IC_{50}/μM
L55	29.6±2.1	41.6±4.1	32.8±6.2	5.0±0.5	27.9±2.8	3.6±0.4
CP4	20.1±2.6	6.9±2.2	>50	>50	24.1±1.9	10.7±1.6

To understand the anti-cancer mechanism of **L55**, we assessed its effects on cell death and the cell cycle in RS4;11 cells. The Annexin-V/PI assay revealed that the ratios of dying cells (Annexin V positive/PI positive, representing late apoptosis or necrosis) increased significantly with the **L55** treatment time (Fig. 5A). Flow cytometry analysis of the cell cycle distribution revealed a time-dependent increase in the subG (apoptotic cell) population, further supporting the cytotoxic effect of **L55**. Moreover, upon **L55** treatment, the proportions of G2/M cells were clearly reduced, while the proportions of G0/G1 and S cells were not apparently altered, suggesting that **L55** might arrest cell progression by restricting the G0/G1 and S phases (Fig. 5B).

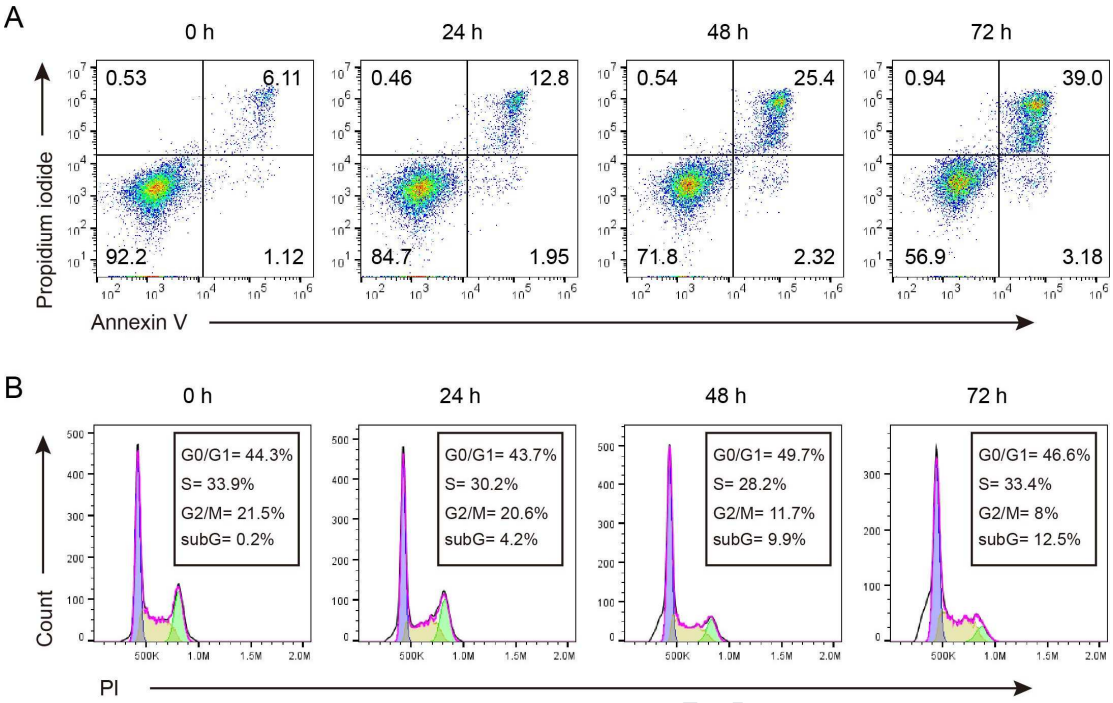

Fig. 5. Effects of **L55** on cell death and cell cycle distribution. (A) Flow cytometric analysis of cell death of RS4;11 cells treated with **L55** (1 μM) for 0 h, 24 h, 48 h or 72 h. (B) The cell cycles of RS4;11 cells were analyzed via flow cytometry after treatment with **L55** (1 μM) for 0 h, 24 h, 48 h or 72 h.

We next assessed the effects of compound **L55** on downstream pathway components of USP7 signaling in RS4;11 cells. As shown in Fig. 6, the protein levels of MDM2 were dose-dependently reduced, while the protein levels of p53 and p21 were increased by **L55** treatment. This result was consistent with the finding that **L55** induced cell death and cell cycle arrest. In addition, another USP7 substrate, DNMT1 (DNA methyltransferase 1), was also downregulated by **L55** in a concentration-dependent manner. Interestingly, **L55** also induced a decrease in the protein level of USP7.

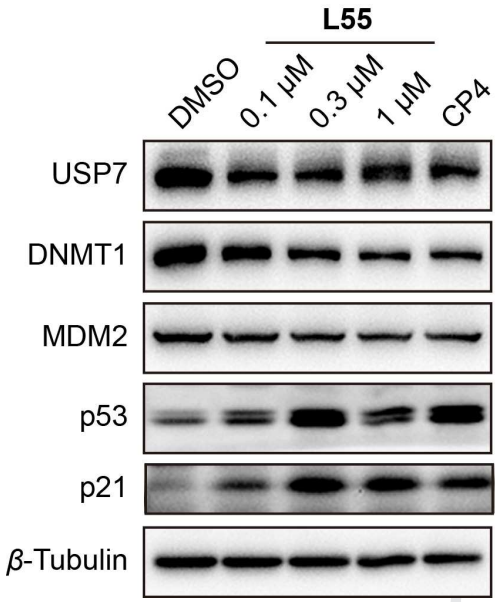

Fig. 6. Effects of **L55** on the protein levels of USP7, DNMT1, MDM2, p53 and p21 in RS4;11 cells. Western blotting analysis of RS4;11 cells treated with **L55**, **CP4** (1 μM) or DMSO for 24 h.

3. CONCLUSIONS

In this study, 55 piperidinol derivatives were designed, synthesized and biologically evaluated to find new USP7 inhibitors. The results of the USP7 inhibitory assay showed that N-benzyl piperidinol derivatives exhibited potent USP7 inhibitory activity, among which compound **L55** was identified as a highly selective and potent USP7 inhibitor (USP7 IC_{50} = 40.8 nM, K_D = 78.3 nM). **L55** showed strong *in vitro* antitumor activity against LNCaP (IC_{50} = 29.6 nM) and RS4;11 (IC_{50} = 41.6 nM) cells. Mechanism studies demonstrated that **L55** caused marked cell death and arrested cell progression through restricting G0/G1 and S phases in RS4;11 cells. Moreover, **L55** dose-dependently reduced the protein levels of oncoproteins MDM2 and DNMT1 and increased the protein levels of tumor suppressors p53 and p21. Interestingly, **L55** also reduced USP7 protein levels in RS4;11 cells. More importantly, the co-crystal structure of USP7 in complex with **L55** revealed that **L55** bound to USP7 at the previously reported site but with a new pose that was very different from the previously reported inhibitors. This co-crystal structure of USP7 in complex with **L55** would assist in the future design of novel structural classes of USP7 inhibitors.

4. Experimental section

4.1 Chemistry

General information General procedures of the synthesis route are described as below. Commercially available reagents and solvents were used without further purification. Analytical thin-layer chromatography (TLC) was performed on silica gel 60 F254 plates (Qingdao Ocean Chemical Company, China). Column chromatography was carried out on silica gel (200-300 mesh, Qingdao Ocean Chemical Company, China). ^{1}H and ^{13}C NMR spectra were recorded on an ACF*300Q Bruker spectrometer with Me_4Si as the internal reference. Proton coupling patterns were described as singlet (s), doublet (d), doublet of doublets (dd), triplet (t), triplet of doublets (td), quartet (q), multiplet (m), and broad (br). Low and high-resolution mass spectra (LRMS and HRMS) were obtained in electrospray ionization mode. The mass analyzer type used for the HRMS measurements was TOF. The melting point (m. p.) was measured on a microscopic melting point apparatus. All compounds underwent UPLC to determine purity immediately before processing the Ub-Rho assays. A Waters Acquity UPLC system comprising the Quaternary Solvent manager, Sample Manager-FTN, PDA Detector were employed. The UPLC conditions were as follows: ACQUITY UPLC® BEH C18 column, 2.1×50 mm, 1.7 μm; detection wavelength: 254 nm.

4.1.1

1-(4-fluorophenyl)-5-((4-hydroxy-1-(pyridin-2-yl)piperidin-4-yl)methyl)-1,5-dihydro-4H-pyrazolo[3,4-d]pyrimidin-4-one (**L1**)

A mixture of **5** (88 mg, 0.2 mmol) [23], 2-bromopyridine (21 μL, 0.22 mmol) and K_2CO_3 (102 mg, 0.74 mmol) in DMF (2 mL) was stirred at 120 °C for 20 h. After cooling to room temperature, the mixture was diluted with water (10 mL), extracted with ethyl acetate (10 mL × 3), and the organic layer was washed with water (10 mL×3) and brine (10 mL), dried over sodium sulfate, filtered and concentrated. The residue was purified by column chromatography (silica gel, petroleum ether : ethyl acetate = 1 : 1) to give compound **L1** (37 mg, 34% yield) as a white solid. m.p.

204-206 °C. ^{1}H NMR (300 MHz, d_6-DMSO) δ 8.42 – 8.32 (m, 2H), 8.12 – 8.04 (m, 3H), 7.54 – 7.37 (m, 3H), 6.86 – 6.79 (m, 1H), 6.61 – 6.53 (m, 1H), 4.90 (s, 1H), 4.05 (s, 2H), 4.00 – 3.90 (m, 2H), 3.26 – 3.16 (m, 2H), 1.64 – 1.53 (m, 2H), 1.48 – 1.39 (m, 2H).ESI-MS: m/z 443.1 $[M+Na]^+$. LC t_R: 0.910 min, purity 97.24%.

4.1.2

1-(4-fluorophenyl)-5-((4-hydroxy-1-(pyrimidin-2-yl)piperidin-4-yl)methyl)-1,5-dihydro-4H-pyrazolo[3,4-d]pyrimidin-4-one (**L2**)

Compound **L2** was prepared according to the procedure described for compound **L1**. **L2**: white solid, 34% yield. m.p. 204-206 °C. ^{1}H NMR (300 MHz, d_6-DMSO) δ 8.42 – 8.30 (m, 4H), 8.15 – 8.00 (m, 2H), 7.51 – 7.35 (m, 2H), 6.62 – 6.54 (m, 1H), 4.96 (s, 1H), 4.37 – 4.26 (m, 2H), 4.06 (s, 2H), 3.29 – 3.23 (m, 2H), 1.64 – 1.37 (m, 4H). ESI-MS: m/z 422.2 $[M+H]^+$. LC t_R: 0.889 min, purity 97.78%.

4.1.3

1-(4-fluorophenyl)-5-((4-hydroxy-1-(quinolin-2-yl)piperidin-4-yl)methyl)-1,5-dihydro-4H-pyrazolo[3,4-d]pyrimidin-4-one (**L3**)

Compound **L3** was prepared according to the procedure described for compound **L1**. **L3**: white solid, 39% yield. m.p. 203-205 °C. ^{1}H NMR (300 MHz, d_6-DMSO) δ 8.38 (s, 1H), 8.37 (s, 1H), 8.14 – 8.05 (m, 2H), 8.04 – 7.97 (m, 1H), 7.72 – 7.65 (m, 1H), 7.59 – 7.49 (m, 2H), 7.50 – 7.38 (m, 2H), 7.30 – 7.15 (m, 2H), 4.96 (s, 1H), 4.31 – 4.14 (m, 2H), 4.06 (s, 2H), 3.46 – 3.33 (m, 2H), 1.75 – 1.56 (m, 2H), 1.56 – 1.41 (m, 2H). ESI-MS: m/z 471.2 $[M+H]^+$. LC t_R: 2.336 min, purity 95.85%.

4.1.4

1-(4-fluorophenyl)-5-((1-(3-fluoropyridin-2-yl)-4-hydroxypiperidin-4-yl)methyl)-1,5-dihydro-4H-pyrazolo[3,4-d]pyrimidin-4-one (**L4**)

Compound **L4** was prepared according to the procedure described for compound **L1**. **L4**: white solid, 39% yield. m.p. 165-167 °C. ^{1}H NMR (300 MHz, d_6-DMSO) δ 8.45 – 8.30 (m, 2H), 8.16 – 7.93 (m, 3H), 7.54 – 7.33 (m, 3H), 6.91 – 6.77 (m, 1H), 4.91 (s,

1H), 4.06 (s, 2H), 3.80 – 3.63 (m, 2H), 3.27 – 3.15 (m, 2H), 1.77 – 1.62 (m, 2H), 1.55 – 1.43 (m, 2H). ESI-MS: m/z 439.1 $[M+H]^+$. LC t_R: 0.597 min, purity 97.42%.

4.1.5

5-((1-(3-chloropyridin-2-yl)-4-hydroxypiperidin-4-yl)methyl)-1-(4-fluorophenyl)-1,5-dihydro-4H-pyrazolo[3,4-d]pyrimidin-4-one (**L5**)

Compound **L5** was prepared according to the procedure described for compound **L1**. **L5**: white solid, 36% yield. m.p. 175-177 °C. ^{1}H NMR (300 MHz, d_6-DMSO) δ 8.46 – 8.31 (m, 2H), 8.24 – 8.15 (m, 1H), 8.15 – 8.01 (m, 2H), 7.81 – 7.71 (m, 1H), 7.51 – 7.36 (m, 2H), 7.03 – 6.89 (m, 1H), 4.87 (s, 1H), 4.08 (s, 2H), 3.57 – 3.40 (m, 2H), 3.22 – 3.04 (m, 2H), 1.86 – 1.66 (m, 2H), 1.60 – 1.44 (m, 2H). ESI-MS: m/z 455.1 $[M+H]^+$. LC t_R: 1.620 min, purity 98.47%.

4.1.6

5-((1-(3-bromopyridin-2-yl)-4-hydroxypiperidin-4-yl)methyl)-1-(4-fluorophenyl)-1,5-dihydro-4H-pyrazolo[3,4-d]pyrimidin-4-one (**L6**)

Compound **L6** was prepared according to the procedure described for compound **L1**. **L6**: white solid, 48% yield. m.p. 171-173 °C. ^{1}H NMR (300 MHz, d_6-DMSO) δ 8.38 (s, 1H), 8.37 (s, 1H), 8.27 – 8.18 (m, 1H), 8.14 – 8.02 (m, 2H), 7.98 – 7.89 (m, 1H), 7.48 – 7.38 (m, 2H), 6.95 – 6.84 (m, 1H), 4.87 (s, 1H), 4.10 (s, 2H), 3.51 – 3.38 (m, 2H), 3.16 – 3.00 (m, 2H), 1.86 – 1.65 (m, 2H), 1.62 – 1.48 (m, 2H). ESI-MS: m/z 455.1 $[M+Na]^+$. LC t_R: 0.900 min, purity 97.56%.

4.1.7

1-(4-fluorophenyl)-5-((4-hydroxy-1-(3-iodopyridin-2-yl)piperidin-4-yl)methyl)-1,5-dihydro-4H-pyrazolo[3,4-d]pyrimidin-4-one (**L7**)

Compound **L7** was prepared according to the procedure described for compound **L1**. **L7**: white solid, 55% yield. m.p. 215-217 °C. ^{1}H NMR (300 MHz, d_6-DMSO) δ 8.41 – 8.35 (m, 2H), 8.29 – 8.22 (m, 1H), 8.19 – 8.12 (m, 1H), 8.12 – 8.04 (m, 2H), 7.50 – 7.36 (m, 2H), 6.81 – 6.71 (m, 1H), 4.86 (s, 1H), 4.10 (s, 2H), 3.41 – 3.31 (m, 2H),

3.14 – 2.98 (m, 2H), 1.88 – 1.68 (m, 2H), 1.64 – 1.45 (m, 2H). ESI-MS: m/z 547.2 $[M+H]^+$. LC t_R: 2.157 min, purity 98.52%.

4.1.8

2-(4-((1-(4-fluorophenyl)-4-oxo-1,4-dihydro-5H-pyrazolo[3,4-d]pyrimidin-5-yl)methyl)-4-hydroxypiperidin-1-yl)nicotinonitrile (**L8**)

Compound **L8** was prepared according to the procedure described for compound **L1**. **L8**: white solid, 48% yield. m.p. 185-187 °C. ^{1}H NMR (300 MHz, d_6-DMSO) δ 8.44 – 8.32 (m, 3H), 8.14 – 7.98 (m, 3H), 7.50 – 7.38 (m, 2H), 6.93 – 6.84 (m, 1H), 4.98 (s, 1H), 4.09 (s, 2H), 4.04 – 3.91 (m, 2H), 3.42 – 3.33 (m, 2H), 1.82 – 1.65 (m, 2H), 1.61 – 1.44 (m, 2H). ESI-MS: m/z 468.1 $[M+Na]^+$. LC t_R: 1.037 min, purity 98.23%.

4.1.9

1-(4-fluorophenyl)-5-((4-hydroxy-1-(6-(trifluoromethyl)pyridin-2-yl)piperidin-4-yl)methyl)-1,5-dihydro-4H-pyrazolo[3,4-d]pyrimidin-4-one (**L9**)

Compound **L9** was prepared according to the procedure described for compound **L1**. **L9**: white solid, 40% yield. m.p. 233-235 °C. ^{1}H NMR (300 MHz, d_6-DMSO) δ 8.43 – 8.32 (m, 2H), 8.14 – 8.01 (m, 2H), 7.79 – 7.65 (m, 1H), 7.53 – 7.38 (m, 2H), 7.20 – 7.07 (m, 1H), 7.04 – 6.93 (m, 1H), 4.97 (s, 1H), 4.06 (s, 2H), 4.05 – 3.96 (m, 2H), 3.29 – 3.18 (m, 2H), 1.70 – 1.56 (m, 2H), 1.53 – 1.38 (m, 2H). ESI-MS: m/z 511.1 $[M+Na]^+$. LC t_R: 2.734 min, purity 96.26%.

4.1.10

2-(4-((1-(4-fluorophenyl)-4-oxo-1,4-dihydro-5H-pyrazolo[3,4-d]pyrimidin-5-yl)methyl)-4-hydroxypiperidin-1-yl)nicotinaldehyde (**L10**)

Compound **L10** was prepared according to the procedure described for compound **L1**. **L10**: white solid, 49% yield. m.p. 172-175 °C. ^{1}H NMR (300 MHz, d_6-DMSO) δ 9.92 (s, 1H), 8.44 – 8.33 (m, 3H), 8.14 – 7.97 (m, 3H), 7.51 – 7.32 (m, 2H), 7.05 – 6.89 (m, 1H), 4.95 (s, 1H), 4.09 (s, 2H), 3.70 – 3.51 (m, 2H), 3.43 – 3.32 (m, 2H), 1.88 – 1.68 (m, 2H), 1.57 – 1.38 (m, 2H). ESI-MS: m/z 471.1 $[M+Na]^+$. LC t_R: 0.912 min, purity 96.41%.

4.1.11

6-(4-((1-(4-fluorophenyl)-4-oxo-1,4-dihydro-5H-pyrazolo[3,4-d]pyrimidin-5-yl)methyl)-4-hydroxypiperidin-1-yl)picolinaldehyde (**L11**)

Compound **L11** was prepared according to the procedure described for compound **L1**. **L11**: white solid, 19% yield. m.p. 170-172 °C. ^{1}H NMR (300 MHz, d_6-DMSO) δ 9.79 (s, 1H), 8.38 (s, 1H), 8.37 (s, 1H), 8.15 – 8.02 (m, 2H), 7.79 – 7.65 (m, 1H), 7.49 – 7.37 (m, 2H), 7.22 – 7.09 (m, 2H), 4.97 (s, 1H), 4.19 – 4.00 (m, 4H), 3.42 – 3.31 (m, 2H), 1.71 – 1.54 (m, 2H), 1.54 – 1.36 (m, 2H). ESI-MS: m/z 471.2 $[M+Na]^+$. LC t_R: 0.445 min, purity 95.78%.

4.1.12

1-(4-fluorophenyl)-5-((4-hydroxy-1-(thiazol-2-yl)piperidin-4-yl)methyl)-1,5-dihydro-4H-pyrazolo[3,4-d]pyrimidin-4-one (**L12**)

A mixture of **5** (221 mg, 0.5 mmol), 2-bromothiazole (82 mg, 0.5 mmol) and K_2CO_3 (138 mg, 1 mmol) in DMF (2 mL) was stirred at 90 °C for 67 h. After cooling to room temperature, the mixture was diluted with water (10 mL), extracted with ethyl acetate (10 mL × 3), and the organic layer was washed with water (10 mL×3) and brine (10 mL), dried over sodium sulfate, filtered and concentrated. The residue was purified by column chromatography (silica gel, DCM: CH_3OH= 1: 1) to give compound **L12** (34 mg, 16% yield) as a white solid. m.p. 210-212 °C. ^{1}H NMR (300 MHz, d_6-DMSO) δ 8.36 (d, J = 2.6 Hz, 2H), 8.18 – 7.99 (m, 2H), 7.42 (t, J = 8.8 Hz, 2H), 7.13 (d, J = 3.6 Hz, 1H), 6.80 (d, J = 3.6 Hz, 1H), 5.00 (s, 1H), 4.06 (s, 2H), 3.77 – 3.59 (m, 2H), 3.28 (t, J = 10.8 Hz, 2H), 1.68 (t, J = 10.2 Hz, 2H), 1.60 – 1.43 (m, 2H). ESI-MS: m/z 449.2 $[M+Na]^+$. LC t_R: 0.856 min, purity 97.06%.

4.1.13 Ethyl

2-(4-((1-(4-fluorophenyl)-4-oxo-1,4-dihydro-5H-pyrazolo[3,4-d]pyrimidin-5-yl)methyl)-4-hydroxypiperidin-1-yl)thiazole-4-carboxylate (**L13**)

Compound **L13** was prepared according to the procedure described for compound **L12**. **L13**: white solid, 18% yield. m.p. 184-186 °C. ^{1}H NMR (300 MHz, d_6-DMSO)

δ 8.35 (d, *J* = 1.8 Hz, 2H), 8.06 (dd, *J* = 8.7, 4.8 Hz, 2H), 7.65 (s, 1H), 7.41 (t, *J* = 8.7 Hz, 2H), 5.01 (s, 1H), 4.21 (q, *J* = 7.0 Hz, 2H), 4.06 (s, 2H), 3.68 (d, *J* = 12.6 Hz, 2H), 1.68 (t, *J* = 10.2 Hz, 2H), 1.58 – 1.41 (m, 2H), 1.25 (t, *J* = 7.0 Hz, 3H). ESI-MS: m/z 521.2 $[M+Na]^+$. LC t_R: 2.779 min, purity 97.84%.

4.1.14

5-((1-benzyl-4-hydroxypiperidin-4-yl)methyl)-1-(4-fluorophenyl)-1,5-dihydro-4H-pyrazolo[3,4-d]pyrimidin-4-one (**L14**)

A mixture of **5** (88 mg, 0.2 mmol), benzyl bromide (36 μL, 0.3 mmol) and K_2CO_3 (102 mg, 0.74 mmol) in DMF (4 mL) was stirred at ambient temperature for 2 h. The mixture was diluted with water (9 mL), extracted with ethyl acetate (6 mL × 3), and the organic layer was washed with water (10 mL×3) and brine (10 mL), dried over sodium sulfate, filtered and concentrated. The residue was purified by column chromatography (silica gel, DCM:methol = 20:1) to give compound **L14** (27 mg, 31% yield) as a light yellow solid. m.p. 178-180 °C. ^{1}H NMR (300 MHz, d_6-DMSO) δ 8.42 – 8.24 (m, 2H), 8.18 – 7.99 (m, 2H), 7.54 – 7.08 (m, 7H), 4.61 (s, 1H), 4.03 (s, 2H), 3.44 (s, 2H), 2.49 – 2.37 (m, 2H), 2.39 – 2.17 (m, 2H), 1.75 – 1.54 (m, 2H), 1.51 – 1.32 (m, 2H). ESI-MS: m/z 434.2 $[M+H]^+$. LC t_R: 1.572 min, purity >99%.

4.1.15

1-(4-fluorophenyl)-5-((4-hydroxy-1-(pyridin-2-ylmethyl)piperidin-4-yl)methyl)-1,5-dihydro-4H-pyrazolo[3,4-d]pyrimidin-4-one (**L15**)

Compound **L15** was prepared according to the procedure described for compound **L14**. **L15**: light yellow solid, 31% yield. m.p. 124-126 °C. ^{1}H NMR (300 MHz, d_6-DMSO) δ 8.54 – 8.40 (m, 1H), 8.40 – 8.28 (m, 2H), 8.16 – 7.95 (m, 2H), 7.85 – 7.64 (m, 1H), 7.52 – 7.32 (m, 3H), 7.28 – 7.15 (m, 1H), 4.66 (s, 1H), 4.01 (s, 2H), 3.57 (s, 2H), 2.64 – 2.50 (m, 2H), 2.44 – 2.24 (m, 2H), 1.72 – 1.51 (m, 2H), 1.47 – 1.28 (m, 2H). ESI-MS: m/z 435.2 $[M+H]^+$. LC t_R: 0.647 min, purity 98.94%.

4.1.16

1-(4-fluorophenyl)-5-((4-hydroxy-1-(pyridin-3-ylmethyl)piperidin-4-yl)methyl)-1,5-d

ihydro-4H-pyrazolo[3,4-d]pyrimidin-4-one (**L16**)

Compound **L16** was prepared according to the procedure described for compound **L14**. **L16**: white solid, 54% yield. m.p. 198-200 °C. ^{1}H NMR (300 MHz, d_6-DMSO) δ 8.54 – 8.40 (m, 2H), 8.37 – 8.27 (m, 2H), 8.14 – 7.98 (m, 2H), 7.77 – 7.62 (m, 1H), 7.51 – 7.22 (m, 3H), 4.66 (s, 1H), 4.00 (s, 2H), 3.47 (s, 2H), 2.60 – 2.49 (m, 2H), 2.38 – 2.19 (m, 2H), 1.70 – 1.49 (m, 2H), 1.48 – 1.28 (m, 2H). ESI-MS: m/z 435.2 $[M+H]^+$. LC t_R: 0.904 min, purity >99%.

4.1.17

1-(4-fluorophenyl)-5-((4-hydroxy-1-(pyridin-4-ylmethyl)piperidin-4-yl)methyl)-1,5-dihydro-4H-pyrazolo[3,4-d]pyrimidin-4-one (**L17**)

Compound **L17** was prepared according to the procedure described for compound **L14**. **L17**: light yellow solid, 61% yield. m.p. 244-246 °C. ^{1}H NMR (300 MHz, d_6-DMSO) δ 8.59 – 8.43 (m, 2H), 8.42 – 8.28 (m, 2H), 8.17 – 8.00 (m, 2H), 7.50 – 7.37 (m, 2H), 7.37 – 7.26 (m, 2H), 4.69 (s, 1H), 4.03 (s, 2H), 3.50 (s, 2H), 3.31 (s, 2H), 2.57 – 2.51 (m, 2H), 2.40 – 2.22 (m, 2H), 1.73 – 1.54 (m, 2H), 1.50 – 1.32 (m, 2H). ESI-MS: m/z 435.2 $[M+H]^+$. LC t_R: 0.912 min, purity 97.69%.

4.1.18 Methyl 2-(2-chlorophenyl)-2-(4-((1-(4-fluorophenyl)-4-oxo-1,4-dihydro-5H-pyrazolo[3,4-d]pyrimidin-5-yl)methyl)-4-hydroxypiperidin-1-yl)acetate (**L18**)

A mixture of **5** (221 mg, 0.5 mmol), methyl 2-bromo-2-(2-chlorophenyl)acetate (131 mg, 0.5 mmol) and K_2CO_3 (138 mg, 1 mmol) in DMF (4 mL) was stirred at ambient temperature for 2 h. The mixture was diluted with water (9 mL), extracted with ethyl acetate (6 mL × 3), and the organic layer was washed with water (10 mL×3) and brine (10 mL), dried over sodium sulfate, filtered and concentrated. The residue was purified by column chromatography (silica gel, DCM : CH_3OH = 20 : 1) to give compound **L18** (150 mg, yield 57%) as a white solid. ^{1}H NMR (300 MHz, d_6-DMSO) δ 8.34 (d, J = 5.5 Hz, 2H), 8.07 (dd, J = 9.0, 4.9 Hz, 2H), 7.58 (d, J = 7.3 Hz, 1H), 7.50 – 7.28 (m, 5H), 4.70 (s, 1H), 4.58 (s, 1H), 4.02 (s, 2H), 3.62 (s, 3H), 2.67 – 2.57

(m, 1H), 2.48 – 2.35 (m, 3H), 1.72 – 1.50 (m, 2H), 1.50 – 1.32 (m, 2H). ESI-MS: m/z 548.2 $[M+Na]^+$. m.p. 168-170 °C. LC t_R: 5.308 min, purity 98.88%.

4.1.19

5-((1-benzhydryl-4-hydroxypiperidin-4-yl)methyl)-1-(4-fluorophenyl)-1,5-dihydro-4H-pyrazolo[3,4-d]pyrimidin-4-one (**L19**)

Compound **L19** was prepared according to the procedure described for compound **L14**. **L19**: white solid, 35% yield. m.p. 220-222 °C. ^{1}H NMR (300 MHz, d_6-DMSO) δ 8.31 (s, 2H), 8.04 (s, 2H), 7.38 (s, 6H), 7.32 – 7.20 (m, 4H), 7.20 – 7.04 (m, 2H), 4.63 (s, 1H), 4.30 (s, 1H), 4.01 (s, 2H), 2.47 – 2.37 (m, 2H), 2.32 – 2.03 (m, 2H), 1.79 – 1.51 (m, 2H), 1.50 – 1.26 (m, 2H). ESI-MS: m/z 532.3 $[M+Na]^+$. LC t_R: 1.083 min, purity 96.31%.

4.1.20

1-(4-fluorophenyl)-5-((4-hydroxy-1-(2-nitrobenzyl)piperidin-4-yl)methyl)-1,5-dihydro-4H-pyrazolo[3,4-d]pyrimidin-4-one (**L20**)

Compound **L20** was prepared according to the procedure described for compound **L14**. **L20**: light yellow solid, 40% yield. m.p. 180-182 °C. ^{1}H NMR (300 MHz, d_6-DMSO) δ 8.35 (s, 1H), 8.33 (s, 1H), 8.13 – 8.00 (m, 2H), 7.88 – 7.79 (m, 1H), 7.70 – 7.57 (m, 2H), 7.57 – 7.36 (m, 3H), 4.67 (s, 1H), 4.00 (s, 2H), 3.71 (s, 2H), 2.47 – 2.21 (m, 4H), 1.64 – 1.44 (m, 2H), 1.42 – 1.27 (m, 2H). ESI-MS: m/z 479.2 $[M+H]^+$. LC t_R: 1.524 min, purity 97.51%.

4.1.21

1-(4-fluorophenyl)-5-((4-hydroxy-1-(3-nitrobenzyl)piperidin-4-yl)methyl)-1,5-dihydro-4H-pyrazolo[3,4-d]pyrimidin-4-one (**L21**)

Compound **L21** was prepared according to the procedure described for compound **L14**. **L21**: white solid, 44% yield. m.p. 90-92 °C. ^{1}H NMR (300 MHz, d_6-DMSO) δ 8.34 (s, 2H), 8.22 – 8.02 (m, 4H), 7.76 (d, J = 7.4 Hz, 1H), 7.62 (t, J = 7.8 Hz, 1H), 7.42 (t, J = 8.7 Hz, 2H), 4.68 (s, 1H), 4.03 (s, 2H), 3.61 (s, 2H), 2.60 – 2.51 (m, 2H), 2.44 – 2.23 (m, 2H), 1.74 – 1.54 (m, 2H), 1.50 – 1.36 (m, 2H). ESI-MS: m/z 479.2

$[M+H]^+$. LC t_R: 1.484 min, purity 94.43%.

4.1.22

1-(4-fluorophenyl)-5-((4-hydroxy-1-(4-nitrobenzyl)piperidin-4-yl)methyl)-1,5-dihydro-4H-pyrazolo[3,4-d]pyrimidin-4-one (**L22**)

Compound **L22** was prepared according to the procedure described for compound **L14**. **L22**: 51% yield as white solid. m.p. 214-216 °C. ^{1}H NMR (300 MHz, d_6-DMSO) δ 8.35 (d, J = 3.5 Hz, 2H), 8.18 (d, J = 8.4 Hz, 2H), 8.07 (dd, J = 8.8, 4.9 Hz, 2H), 7.59 (d, J = 8.4 Hz, 2H), 7.42 (t, J = 8.8 Hz, 2H), 4.69 (s, 1H), 4.03 (s, 2H), 3.60 (s, 2H), 2.57 – 2.51 (m, 2H), 2.33 (t, J = 10.2 Hz, 2H), 1.63 (t, J = 10.1 Hz, 2H), 1.41 (d, J = 12.9 Hz, 2H). ESI-MS: m/z 479.2 $[M+H]^+$. LC t_R:1.444 min, purity 93.09%.

4.1.23

5-((1-(2-fluorobenzyl)-4-hydroxypiperidin-4-yl)methyl)-1-(4-fluorophenyl)-1,5-dihydro-4H-pyrazolo[3,4-d]pyrimidin-4-one (**L23**)

Compound **L23** was prepared according to the procedure described for compound **L14**. **L23**: white solid, 53% yield. m.p. 174-176 °C. ^{1}H NMR (300 MHz, d_6-DMSO) δ 8.35 (s, 1H), 8.33 (s, 1H), 8.11 – 8.01 (m, 2H), 7.48 – 7.36 (m, 3H), 7.35 – 7.25 (m, 1H), 7.20 – 7.09 (m, 2H), 4.65 (s, 1H), 4.01 (s, 2H), 3.58 – 3.45 (m, 2H), 2.39 – 2.25 (m, 2H), 1.65 – 1.54 (m, 2H), 1.41 – 1.33 (m, 2H). ESI-MS: m/z 452.2 $[M+H]^+$. LC t_R: 1.216 min, purity 97.49%.

4.1.24

5-((1-(4-fluorobenzyl)-4-hydroxypiperidin-4-yl)methyl)-1-(4-fluorophenyl)-1,5-dihydro-4H-pyrazolo[3,4-d]pyrimidin-4-one (**L24**)

Compound **L24** was prepared according to the procedure described for compound **L14**. **L24**: white solid, 58% yield. m.p. 206-208 °C. ^{1}H NMR (300 MHz, d_6-DMSO) δ 8.35 (s, 1H), 8.34 (s, 1H), 8.13 – 8.01 (m, 2H), 7.50 – 7.37 (m, 2H), 7.38 – 7.24 (m, 2H), 7.19 – 7.06 (m, 2H), 4.66 (s, 1H), 4.02 (s, 2H), 3.44 (s, 2H), 2.49 – 2.44 (m, 2H), 2.33 – 2.19 (m, 2H), 1.71 – 1.50 (m, 2H), 1.48 – 1.30 (m, 2H). ESI-MS: m/z 452.3 $[M+H]^+$. LC t_R: 0.933 min, purity 96.77%.

4.1.25

5-((1-(2-chlorobenzyl)-4-hydroxypiperidin-4-yl)methyl)-1-(4-fluorophenyl)-1,5-dihydro-4H-pyrazolo[3,4-d]pyrimidin-4-one (**L25**)

Compound **L25** was prepared according to the procedure described for compound **L14**. **L25**: white solid, 48% yield. m.p. 218-220 °C. ^{1}H NMR (300 MHz, d_6-DMSO) δ 8.36 (s, 1H), 8.34 (s, 1H), 8.14 – 8.00 (m, 2H), 7.54 – 7.37 (m, 4H), 7.37 – 7.20 (m, 2H), 4.69 (s, 1H), 4.03 (s, 2H), 3.55 (s, 2H), 2.62 – 2.52 (m, 2H), 2.43 – 2.30 (m, 2H), 1.69 – 1.54 (m, 2H), 1.47 – 1.34 (m, 2H). ESI-MS: m/z 468.2 $[M+H]^+$. LC t_R: 1.411 min, purity 96.24%.

4.1.26

5-((1-(3-chlorobenzyl)-4-hydroxypiperidin-4-yl)methyl)-1-(4-fluorophenyl)-1,5-dihydro-4H-pyrazolo[3,4-d]pyrimidin-4-one (**L26**)

Compound **L26** was prepared according to the procedure described for compound **L14**. **L26**: white solid, 65% yield. m.p. 194-196 °C. ^{1}H NMR (300 MHz, d_6-DMSO) δ 8.35 (s, 1H), 8.34 (s, 1H), 8.13 – 7.99 (m, 2H), 7.50 – 7.21 (m, 6H), 4.66 (s, 1H), 4.02 (s, 2H), 3.47 (s, 2H), 2.49 – 2.45 (m, 2H), 2.36 – 2.22 (m, 2H), 1.68 – 1.53 (m, 2H), 1.46 – 1.33 (m, 2H). ESI-MS: m/z 468.1$[M+H]^+$. LC t_R: 1.139 min, purity 95.44%.

4.1.27

5-((1-(4-chlorobenzyl)-4-hydroxypiperidin-4-yl)methyl)-1-(4-fluorophenyl)-1,5-dihydro-4H-pyrazolo[3,4-d]pyrimidin-4-one (**L27**)

Compound **L27** was prepared according to the procedure described for compound **L14**. **L27**: white solid, 39% yield. m.p. 224-226 °C. ^{1}H NMR (300 MHz, d_6-DMSO) δ 8.47 – 8.25 (m, 2H), 8.18 – 7.95 (m, 2H), 7.68 – 7.20 (m, 6H), 4.67 (s, 1H), 4.03 (s, 2H), 3.44 (s, 2H), 2.49 – 2.41 (m, 2H), 2.36 – 2.16 (m, 2H), 1.72 – 1.52 (m, 2H), 1.47 – 1.31 (m, 2H). ESI-MS: m/z 468.2 $[M+H]^+$. LC t_R: 2.271 min, purity >99%.

4.1.28

5-((1-(2-bromobenzyl)-4-hydroxypiperidin-4-yl)methyl)-1-(4-fluorophenyl)-1,5-dihydro-4H-pyrazolo[3,4-d]pyrimidin-4-one (**L28**)

Compound **L28** was prepared according to the procedure described for compound **L14**. **L28**: white solid, 41% yield. m.p. 214-216 °C. ^{1}H NMR (300 MHz, d_6-DMSO) δ 8.46 – 8.24 (m, 2H), 8.19 – 7.94 (m, 2H), 7.65 – 7.53 (m, 1H), 7.53 – 7.26 (m, 4H), 7.27 – 7.10 (m, 1H), 4.68 (s, 1H), 4.03 (s, 2H), 3.52 (s, 2H), 2.61 – 2.53 (m, 2H), 2.45 – 2.27 (m, 2H), 1.75 – 1.52 (m, 2H), 1.49 – 1.31 (m, 2H). ESI-MS: m/z 512.2 $[M+H]^+$. LC t_R: 2.580 min, purity 97.52%.

4.1.29

5-((1-(4-bromobenzyl)-4-hydroxypiperidin-4-yl)methyl)-1-(4-fluorophenyl)-1,5-dihydro-4H-pyrazolo[3,4-d]pyrimidin-4-one (**L29**)

Compound **L29** was prepared according to the procedure described for compound **L14**. **L29**: white solid, 72% yield. m.p. 208-210 °C. ^{1}H NMR (300 MHz, d_6-DMSO) δ 8.35 (s, 1H), 8.33 (s, 1H), 8.13 – 8.01 (m, 2H), 7.54 – 7.37 (m, 4H), 7.31 – 7.21 (m, 2H), 4.65 (s, 1H), 4.02 (s, 2H), 3.43 (s, 2H), 2.49 – 2.42 (m, 2H), 2.34 – 2.19 (m, 2H), 1.65 – 1.51 (m, 2H), 1.44 – 1.35 (m, 2H). ESI-MS: m/z 512.2 $[M+H]^+$. LC t_R: 1.202 min, purity 95.07%.

4.1.30

2-((4-((1-(4-fluorophenyl)-4-oxo-1,4-dihydro-5H-pyrazolo[3,4-d]pyrimidin-5-yl)methyl)-4-hydroxypiperidin-1-yl)methyl)benzonitrile (**L30**)

Compound **L30** was prepared according to the procedure described for compound **L14**. **L30**: white solid, 45% yield. m.p. 184-186 °C. ^{1}H NMR (300 MHz, d_6-DMSO) δ 8.44 – 8.26 (m, 2H), 8.14 – 7.99 (m, 2H), 7.84 – 7.75 (m, 1H), 7.73 – 7.62 (m, 1H), 7.62 – 7.53 (m, 1H), 7.51 – 7.33 (m, 3H), 4.72 (s, 1H), 4.02 (s, 2H), 3.65 (s, 2H), 2.62 – 2.52 (m, 2H), 2.45 – 2.29 (m, 2H), 1.68 – 1.50 (m, 2H), 1.49 – 1.33 (m, 2H). ESI-MS: m/z 459.2 $[M+H]^+$. LC t_R: 1.211 min, purity 97.71%.

4.1.31

4-((4-((1-(4-fluorophenyl)-4-oxo-1,4-dihydro-5H-pyrazolo[3,4-d]pyrimidin-5-yl)methyl)-4-hydroxypiperidin-1-yl)methyl)benzonitrile (**L31**)

Compound **L31** was prepared according to the procedure described for compound

L14. **L31**: white solid, 22% yield. m.p. 204-206 °C. ^{1}H NMR (300 MHz, d_6-DMSO) δ 8.36 (s, 1H), 8.34 (s, 1H), 8.15 – 8.01 (m, 2H), 7.85 – 7.70 (m, 2H), 7.58 – 7.34 (m, 4H), 4.68 (s, 1H), 4.02 (s, 2H), 3.55 (s, 2H), 2.64 – 2.52 (m, 2H), 2.40 – 2.23 (m, 2H), 1.69 – 1.51 (m, 2H), 1.50 – 1.31 (m, 2H). ESI-MS: m/z 459.2 $[M+H]^+$. LC t_R: 1.141 min, purity 96.61%.

4.1.32

1-(4-fluorophenyl)-5-((4-hydroxy-1-(4-(trifluoromethyl)benzyl)piperidin-4-yl)methyl)-1,5-dihydro-4H-pyrazolo[3,4-d]pyrimidin-4-one (**L32**)

Compound **L32** was prepared according to the procedure described for compound **L1**. **L32**; white solid, 36% yield. m.p. 177-179 °C. ^{1}H NMR (300 MHz, d_6-DMSO) δ 8.35 (s, 1H), 8.34 (s, 1H), 8.14 – 8.01 (m, 2H), 7.74 – 7.62 (m, 2H), 7.58 – 7.48 (m, 2H), 7.48 – 7.35 (m, 2H), 4.67 (s, 1H), 4.03 (s, 2H), 3.56 (s, 2H), 2.49 – 2.44 (m, 2H), 2.42 – 2.17 (m, 2H), 1.72 – 1.51 (m, 2H), 1.51 – 1.32 (m, 2H). ESI-MS: m/z 502.2 $[M+H]^+$. LC t_R: 1.153 min, purity 96.15%.

4.1.33

1-(4-fluorophenyl)-5-((4-hydroxy-1-(2-methylbenzyl)piperidin-4-yl)methyl)-1,5-dihydro-4H-pyrazolo[3,4-d]pyrimidin-4-one (**L33**)

Compound **L33** was prepared according to the procedure described for compound **L14**. **L33**: white solid, 32% yield. m.p. 204-206 °C. ^{1}H NMR (300 MHz, d_6-DMSO) δ 8.36 (s, 2H), 8.07 (dd, J = 8.8, 4.8 Hz, 2H), 7.43 (t, J = 8.7 Hz, 2H), 7.17 (d, J = 24.0 Hz, 4H), 4.68 (s, 1H), 4.03 (s, 2H), 3.40 (s, 2H), 3.32 (s, 3H), 2.31 (s, 4H), 1.56 (d, J = 8.8 Hz, 2H), 1.39 (d, J = 10.4 Hz, 2H). ESI-MS: m/z 448.2 $[M+H]^+$. LC t_R: 2.364 min, purity 97.34%.

4.1.34

1-(4-fluorophenyl)-5-((4-hydroxy-1-(4-methylbenzyl)piperidin-4-yl)methyl)-1,5-dihydro-4H-pyrazolo[3,4-d]pyrimidin-4-one (**L34**)

Compound **L34** was prepared according to the procedure described for compound

L14. **L34**: white solid, 60% yield. m.p. 200-202 °C. ^{1}H NMR (300 MHz, d_6-DMSO) δ 8.35 (s, 1H), 8.34 (s, 1H), 8.15 – 7.99 (m, 2H), 7.74 – 7.65 (m, 1H), 7.49 – 7.34 (m, 2H), 7.24 – 7.03 (m, 3H), 4.64 (s, 1H), 4.01 (s, 2H), 3.41 (s, 2H), 2.49 – 2.42 (m, 2H), 2.38 – 2.12 (m, 5H), 1.65 – 1.54 (m, 2H), 1.43 – 1.35 (m, 2H). ESI-MS: m/z 448.2 $[M+H]^+$. LC t_R: 1.420 min, purity 97.13%.

4.1.35 Methyl 2-((4-((1-(4-fluorophenyl)-4-oxo-1,4-dihydro-5H-pyrazolo[3,4-d]pyrimidin-5-yl)methyl)-4-hydroxypiperidin-1-yl)methyl)benzoate (**L35**)

Compound **L35** was prepared according to the procedure described for compound **L14**. **L35**: white solid, 57% yield. m.p. 180-182 °C. ^{1}H NMR (300 MHz, d_6-DMSO) δ 8.32 (d, *J* = 5.4 Hz, 2H), 8.05 (dd, *J* = 8.8, 4.9 Hz, 2H), 7.55 (d, *J* = 7.4 Hz, 1H), 7.49 – 7.26 (m, 5H), 4.65 (s, 1H), 3.98 (s, 2H), 3.77 (s, 3H), 3.62 (s, 2H), 2.43 – 2.31 (m, 2H), 2.25 (t, *J* = 9.8 Hz, 2H), 1.50 (t, *J* = 9.8 Hz, 2H), 1.40 – 1.26 (m, 2H). ESI-MS: m/z 492.2 $[M+H]^+$. LC t_R: 1.330 min, purity 96.44%.

4.1.36 Methyl 3-((4-((1-(4-fluorophenyl)-4-oxo-1,4-dihydro-5H-pyrazolo[3,4-d]pyrimidin-5-yl)methyl)-4-hydroxypiperidin-1-yl)methyl)benzoate (**L36**)

Compound **L36** was prepared according to the procedure described for compound **L14**. **L36**: white solid, 63% yield. m.p. 158-160 °C. ^{1}H NMR (300 MHz, d_6-DMSO) δ 8.33 (d, *J* = 3.5 Hz, 2H), 8.05 (dd, *J* = 8.8, 4.9 Hz, 2H), 7.88 (s, 1H), 7.82 (d, *J* = 7.4 Hz, 1H), 7.55 (d, *J* = 7.2 Hz, 1H), 7.50 – 7.32 (m, 3H), 4.65 (s, 1H), 4.01 (s, 2H), 3.84 (s, 3H), 3.51 (s, 2H), 2.49 (s, 2H), 2.30 (d, *J* = 9.8 Hz, 2H), 1.57 (d, *J* = 9.6 Hz, 2H), 1.47 – 1.28 (m, 2H). ESI-MS: m/z 492.3 $[M+H]^+$. LC t_R: 1.146 min, purity 97.29%.

4.1.37 Methyl 4-((4-((1-(4-fluorophenyl)-4-oxo-1,4-dihydro-5H-pyrazolo[3,4-d]pyrimidin-5-yl)methyl)-4-hydroxypiperidin-1-yl)methyl)benzoate (**L37**)

Compound **L37** was prepared according to the procedure described for compound **L14**. **L24**: white solid, 57% yield. m.p. 186-188 °C. ^{1}H NMR (300 MHz, d_6-DMSO)

δ 8.33 (d, *J* = 2.5 Hz, 2H), 8.05 (dd, *J* = 8.6, 4.8 Hz, 2H), 7.89 (d, *J* = 7.8 Hz, 2H), 7.49 – 7.31 (m, 4H), 4.65 (s, 1H), 4.01 (s, 2H), 3.82 (s, 3H), 3.52 (s, 2H), 2.49 (s, 2H), 2.29 (t, *J* = 9.9 Hz, 2H), 1.60 (t, *J* = 10.1 Hz, 2H), 1.47 – 1.30 (m, 2H). ESI-MS: m/z 492.3 $[M+H]^+$. LC t_R: 1.133 min, purity 98.15%.

4.1.38

5-((1-(3,5-difluorobenzyl)-4-hydroxypiperidin-4-yl)methyl)-1-(4-fluorophenyl)-1,5-dihydro-4H-pyrazolo[3,4-d]pyrimidin-4-one (**L38**)

Compound **L38** was prepared according to the procedure described for compound **L14**. **L38**: white solid, 77% yield. m.p. 206-208 °C. ^{1}H NMR (300 MHz, d_6-DMSO) δ 8.35 (s, 1H), 8.32 (s, 1H), 8.14 – 8.01 (m, 2H), 7.53 – 7.28 (m, 3H), 7.16 – 7.00 (m, 2H), 4.63 (s, 1H), 3.99 (s, 2H), 3.56 (s, 2H), 2.49 – 2.45 (m, 2H), 2.44 – 2.19 (m, 2H), 1.66 – 1.46 (m, 2H), 1.46 – 1.31 (m, 2H). ESI-MS: m/z 470.3$[M+H]^+$. LC t_R: 0.922 min, purity 97.13%.

4.1.39

5-((1-(2,6-dichlorobenzyl)-4-hydroxypiperidin-4-yl)methyl)-1-(4-fluorophenyl)-1,5-dihydro-4H-pyrazolo[3,4-d]pyrimidin-4-one (**L39**)

Compound **L39** was prepared according to the procedure described for compound **L14**. **L39**: white solid, 42% yield. m.p. 242-244 °C. ^{1}H NMR (300 MHz, d_6-DMSO) δ 8.34 (d, *J* = 6.9 Hz, 2H), 8.07 (dd, *J* = 8.8, 4.9 Hz, 2H), 7.50 – 7.26 (m, 5H), 4.69 (s, 1H), 4.00 (s, 2H), 3.66 (s, 2H), 2.50 – 2.36 (m, 4H), 1.62 – 1.44 (m, 2H), 1.43 – 1.31 (m, 2H). ESI-MS: m/z 502.2 $[M+H]^+$. LC t_R:1.636 min, purity 95.79%.

4.1.40

5-((1-(2-chloro-4-fluorobenzyl)-4-hydroxypiperidin-4-yl)methyl)-1-(4-fluorophenyl)-1,5-dihydro-4H-pyrazolo[3,4-d]pyrimidin-4-one (**L40**)

Compound **L40** was prepared according to the procedure described for compound **L14**. **L40**: white solid, 46% yield. m.p. 214-216 °C. ^{1}H NMR (300 MHz, d_6-DMSO) δ 8.36 (s, 1H), 8.34 (s, 1H), 8.14 – 7.98 (m, 2H), 7.77 – 7.32 (m, 4H), 7.27 – 7.12 (m, 1H), 4.69 (s, 1H), 4.03 (s, 2H), 3.51 (s, 2H), 2.61 – 2.51 (m, 2H), 2.43 – 2.28 (m, 2H),

1.66 – 1.54 (m, 2H), 1.44 – 1.34 (m, 2H). ESI-MS: m/z 486.2 $[M+H]^+$. LC t_R: 1.255 min, purity 95.59%.

4.1.41

5-((1-(2,4-dichlorobenzyl)-4-hydroxypiperidin-4-yl)methyl)-1-(4-fluorophenyl)-1,5-dihydro-4H-pyrazolo[3,4-d]pyrimidin-4-one (**L41**)

Compound **L41** was prepared according to the procedure described for compound **L14**. **L41**: white solid, 47% yield. m.p. 198-200 °C. ^{1}H NMR (300 MHz, d_6-DMSO) δ 8.45 – 8.26 (m, 2H), 8.16 – 7.96 (m, 2H), 7.67 – 7.26 (m, 5H), 4.69 (s, 1H), 4.04 (s, 2H), 3.53 (s, 2H), 2.61 – 2.51 (m, 2H), 2.45 – 2.25 (m, 2H), 1.77 – 1.53 (m, 2H), 1.53 – 1.33 (m, 2H). ESI-MS: m/z 502.2 $[M+H]^+$. LC t_R: 1.716 min, purity >99%.

4.1.42

5-((1-(4-bromo-2-chlorobenzyl)-4-hydroxypiperidin-4-yl)methyl)-1-(4-fluorophenyl)-1,5-dihydro-4H-pyrazolo[3,4-d]pyrimidin-4-one (**L42**)

Compound **L42** was prepared according to the procedure described for compound **L14**. **L42**: white solid, 40% yield. m.p. 184-186 °C. ^{1}H NMR (300 MHz, d_6-DMSO) δ 8.36 (s, 1H), 8.34 (s, 1H), 8.13 – 8.00 (m, 2H), 7.74 – 7.62 (m, 1H), 7.58 – 7.49 (m, 1H), 7.49 – 7.36 (m, 3H), 4.70 (s, 1H), 4.03 (s, 2H), 3.51 (s, 2H), 2.62 – 2.52 (m, 2H), 2.44 – 2.22 (m, 2H), 1.74 – 1.52 (m, 2H), 1.53 – 1.33 (m, 2H). ESI-MS: m/z 546.1$[M+H]^+$. LC t_R: 1.853 min, purity 95.09%.

4.1.43 Methyl 3-fluoro-4-((4-((1-(4-fluorophenyl)-4-oxo-1,4-dihydro-5H-pyrazolo[3,4-d]pyrimidin-5-yl)methyl)-4-hydroxypiperidin-1-yl)methyl)benzoate (**L43**)

Compound **L43** was prepared according to the procedure described for compound **L14**. **L43**: white solid, 32% yield. m.p. 185-187 °C. ^{1}H NMR (300 MHz, d_6-DMSO) δ 8.36 (s, 1H), 8.34 (s, 1H), 8.17 – 8.00 (m, 2H), 7.87 – 7.72 (m, 1H), 7.74 – 7.54 (m, 2H), 7.51 – 7.31 (m, 2H), 4.68 (s, 1H), 4.02 (s, 2H), 3.86 (s, 3H), 3.58 (s, 2H), 2.63 – 2.52 (m, 2H), 2.42 – 2.19 (m, 2H), 1.72 – 1.54 (m, 2H), 1.48 – 1.31 (m, 2H). ESI-MS: m/z 510.2$[M+H]^+$. LC t_R: 0.671 min, purity > 99%.

4.1.44 Methyl 3-chloro-4-((4-((1-(4-fluorophenyl)-4-oxo-1,4-dihydro-5H-pyrazolo[3,4-d]pyrimidin-5-yl)methyl)-4-hydroxypiperidin-1-yl)methyl)benzoate (**L44**)

Compound **L44** was prepared according to the procedure described for compound **L14**. **L44**: white solid, 50% yield. m.p. 168-170 °C. ^{1}H NMR (300 MHz, d_6-DMSO) δ 8.35 (d, *J* = 3.0 Hz, 2H), 8.07 (dd, *J* = 8.7, 4.8 Hz, 2H), 7.99 – 7.85 (m, 2H), 7.66 (d, *J* = 8.3 Hz, 1H), 7.42 (t, *J* = 8.7 Hz, 2H), 4.71 (s, 1H), 4.03 (s, 2H), 3.86 (s, 3H), 3.61 (s, 2H), 2.62 – 2.52 (m, 2H), 2.45 – 2.33 (m, 2H), 1.73 – 1.55 (m, 2H), 1.49 – 1.35 (m, 2H). ESI-MS: m/z 526.2 $[M+H]^+$. LC t_R: 0.865 min, purity > 99%.

4.1.45 Methyl 3-bromo-4-((4-((1-(4-fluorophenyl)-4-oxo-1,4-dihydro-5H-pyrazolo[3,4-d]pyrimidin-5-yl)methyl)-4-hydroxypiperidin-1-yl)methyl)benzoate (**L45**)

Compound **L45** was prepared according to the procedure described for compound **L14**. **L45**: white solid, 49% yield. m.p. 133-135 °C. ^{1}H NMR (300 MHz, d_6-DMSO) δ 8.36 (s, 1H), 8.35 (s, 1H), 8.13 – 8.03 (m, 3H), 7.99 – 7.92 (m, 1H), 7.69 – 7.62 (m, 1H), 7.48 – 7.37 (m, 2H), 4.72 (s, 1H), 4.04 (s, 2H), 3.86 (s, 3H), 3.59 (s, 2H), 2.65 – 2.54 (m, 2H), 2.45 – 2.32 (m, 2H), 1.73 – 1.57 (m, 2H), 1.50 – 1.35 (m, 2H). ESI-MS: m/z 570.1$[M+H]^+$. LC t_R: 0.931 min, purity > 99%.

4.1.46 5-((1-(4-chloro-2-(trifluoromethyl)benzyl)-4-hydroxypiperidin-4-yl)methyl)-1-(4-fluorophenyl)-1,5-dihydro-4H-pyrazolo[3,4-d]pyrimidin-4-one (**L46**)

Compound **L46** was prepared according to the procedure described for compound **L14**. **L46**: white solid, 86% yield. m.p. 198-200 °C. ^{1}H NMR (300 MHz, d_6-DMSO) δ 8.35 (d, *J* = 3.7 Hz, 2H), 8.17 – 7.99 (m, 2H), 7.86 – 7.78 (m, 1H), 7.78 – 7.68 (m, 2H), 7.42 (t, *J* = 8.7 Hz, 2H), 4.71 (s, 1H), 4.03 (s, 2H), 3.58 (s, 2H), 2.56 – 2.50 (m, 2H), 2.40 – 2.21 (m, 2H), 1.76 – 1.52 (m, 2H), 1.50 – 1.32 (m, 2H). ESI-MS: m/z 536.2 $[M+H]^+$. LC t_R: 1.511 min, purity 98.25%.

4.1.47

5-chloro-2-((4-((1-(4-fluorophenyl)-4-oxo-1,4-dihydro-5H-pyrazolo[3,4-d]pyrimidin-5-yl)methyl)-4-hydroxypiperidin-1-yl)methyl)benzonitrile (**L47**)

Compound **L47** was prepared according to the procedure described for compound **L14**. **L47**: white solid, 44% yield. m.p. 208-210 °C. ^{1}H NMR (300 MHz, d_6-DMSO) δ 8.35 (s, 1H), 8.34 (s, 1H), 8.12 – 8.02 (m, 2H), 8.01 – 7.95 (m, 1H), 7.78 – 7.70 (m, 1H), 7.62 – 7.56 (m, 1H), 7.47 – 7.37 (m, 2H), 4.70 (s, 1H), 4.02 (s, 2H), 3.61 (s, 2H), 2.57 – 2.51 (m, 2H), 2.44 – 2.32 (m, 2H), 1.68 – 1.50 (m, 2H), 1.48 – 1.32 (m, 2H). ESI-MS: m/z 515.2$[M+Na]^+$. LC t_R: 0.727 min, purity > 99%.

4.1.48

3-bromo-4-((4-((1-(4-fluorophenyl)-4-oxo-1,4-dihydro-5H-pyrazolo[3,4-d]pyrimidin-5-yl)methyl)-4-hydroxypiperidin-1-yl)methyl)benzonitrile (**L48**)

Compound **L48** was prepared according to the procedure described for compound **L14**. **L48**: white solid, 64% yield. m.p. 228-230 °C. ^{1}H NMR (300 MHz, d_6-DMSO) δ 8.34 (s, 2H), 8.14 (s, 1H), 8.12 – 7.99 (m, 2H), 7.85 (d, J = 7.8 Hz, 1H), 7.67 (d, J = 7.8 Hz, 1H), 7.42 (t, J = 8.3 Hz, 2H), 4.71 (s, 1H), 4.03 (s, 2H), 3.58 (s, 2H), 2.61 – 2.51 (m, 2H), 2.46 – 2.30 (m, 2H), 1.73 – 1.53 (m, 2H), 1.51 – 1.34 (m, 2H). ESI-MS: m/z 537.2 539.2 $[M+H]^+$. LC t_R: 1.558 min, purity 96.17%.

4.1.49

3-chloro-4-((4-((1-(4-fluorophenyl)-4-oxo-1,4-dihydro-5H-pyrazolo[3,4-d]pyrimidin-5-yl)methyl)-4-hydroxypiperidin-1-yl)methyl)benzoate (**L49**)

Compound **L49** was prepared according to the procedure described for compound **L14**. **L49**: white solid, 58% yield. m.p. 168-170 °C. ^{1}H NMR (300 MHz, d_6-DMSO) δ 8.34 (d, J = 3.6 Hz, 2H), 8.06 (dd, J = 9.1, 4.9 Hz, 2H), 7.95 – 7.82 (m, 2H), 7.65 (d, J = 8.4 Hz, 1H), 7.41 (t, J = 8.8 Hz, 2H), 4.70 (s, 1H), 4.31 (q, J = 7.1 Hz, 2H), 4.03 (s, 2H), 3.60 (s, 2H), 2.54 (d, J = 11.5 Hz, 2H), 2.38 (t, J = 10.1 Hz, 2H), 1.63 (t, J = 10.4 Hz, 2H), 1.41 (d, J = 13.1 Hz, 2H), 1.31 (t, J = 7.1 Hz, 3H). ESI-MS: m/z 562.2 $[M+Na]^+$. LC t_R: 1.047 min, purity > 99%.

4.1.50

3-chloro-4-((4-((1-(4-fluorophenyl)-4-oxo-1,4-dihydro-5H-pyrazolo[3,4-d]pyrimidin-5-yl)methyl)-4-hydroxypiperidin-1-yl)methyl)benzoic acid (**L50**)

To the solution of **L44** (50 mg, 0.095 mmol) in MeOH (2 mL) was added 50% NH_2OH aqueous solution (2 mL). The resulting mixture was heated in a sealed tube at 90 °C for 5 h and concentrated under reduced pressure. The residue was purified by column chromatography (silica gel, DCM : MeOH = 5 : 1) to give compound **L50** (35 mg, 73% yield) as a white solid. m.p. 206-208 °C. ^{1}H NMR (300 MHz, d_6-DMSO) δ 8.35 (d, *J* = 3.4 Hz, 2H), 8.06 (dd, *J* = 9.0, 4.8 Hz, 2H), 7.89 (s, 1H), 7.82 (d, *J* = 7.9 Hz, 1H), 7.50 – 7.33 (m, 3H), 4.76 (s, 1H), 4.03 (s, 2H), 3.54 (s, 2H), 2.60 – 2.51 (m, 2H), 2.42 – 2.22 (m, 2H), 1.73 – 1.52 (m, 2H), 1.48 – 1.33 (m, 2H). ESI-MS: m/z 512.2 $[M+H]^+$. LC t_R: 0.384 min, purity 98.21%.

4.1.51

3-chloro-4-((4-((1-(4-fluorophenyl)-4-oxo-1,4-dihydro-5H-pyrazolo[3,4-d]pyrimidin-5-yl)methyl)-4-hydroxypiperidin-1-yl)methyl)benzamide (**L51**)

To the solution of **L50** (30 mg, 0.059 mmol) in DCM (3 mL) was added oxalyl chloride (110 μL, 1.3 mmol) and 1 drop of DMF. The resulting solution was stirred at room temperature for 1.5 h and concentrated. The residue was dissolved in DCM (2.5 mL) and added dropwise to ammonia methanol solution (2 mL). The solution was stirred for 2 h and concentrated. The residue was purified by column chromatography (silica gel, DCM : MeOH = 10 : 1) to give compound **L51** (9 mg, 30% yield) as a white solid. m.p. 250-252 °C. ^{1}H NMR (300 MHz, d_6-DMSO) δ 8.36 (s, 1H), 8.35 (s, 1H), 8.18 – 7.98 (m, 3H), 7.91 (s, 1H), 7.82 (d, *J* = 7.9 Hz, 1H), 7.57 (d, *J* = 7.9 Hz, 1H), 7.51 – 7.37 (m, 3H), 4.70 (s, 1H), 4.04 (s, 2H), 3.59 (s, 2H), 2.64 – 2.53 (m, 2H), 2.38 (t, *J* = 10.2 Hz, 2H), 1.63 (t, *J* = 10.0 Hz, 2H), 1.51 – 1.33 (m, 2H). ESI-MS: m/z 511.2 $[M+H]^+$. LC t_R: 0.881 min, purity 97.95%.

4.1.52

3-chloro-4-((4-((1-(4-fluorophenyl)-4-oxo-1,4-dihydro-5H-pyrazolo[3,4-d]pyrimidin-5-yl)methyl)-4-hydroxypiperidin-1-yl)methyl)-N-methylbenzamide (**L52**)

To the solution of **L50** (35 mg, 0.068 mmol) in DMF (4 mL) was added DIPEA (45 μL, 0.272 mmol) and HATU (28 mg, 0.0748 mmol). The mixture was stirred at ambient temperature for 15 min in a sealed tube. To the solution was added 27% methylamine EtOH solution (1 mL). After stirring for 28 h, the reaction was quenched by the addition of H_2O (10 mL), and the mixture was extracted with ethyl acetate (3×10 mL). The combined organic layers were washed with water and dried over Na_2SO_4. After removal of solvent by evaporation, the crude product was purified by column chromatography (silica gel, DCM : CH_3OH = 30 : 1) to give compound **L52** (14 mg, 40% yield) as a white solid. 40% yield. m.p. 222-224 °C. ^{1}H NMR (300 MHz, d_6-DMSO) δ 8.50 (s, 1H), 8.34 (d, *J* = 4.0 Hz, 2H), 8.15 – 8.00 (m, 2H), 7.85 (s, 1H), 7.77 (d, *J* = 7.1 Hz, 1H), 7.56 (d, *J* = 8.0 Hz, 1H), 7.42 (t, *J* = 8.8 Hz, 2H), 4.69 (s, 1H), 4.03 (s, 2H), 3.57 (s, 2H), 2.77 (d, *J* = 4.0 Hz, 3H), 2.62 – 2.50 (m, 2H), 2.44 – 2.24 (m, 2H), 1.77 – 1.54 (m, 2H), 1.50 – 1.34 (m, 2H). ESI-MS: m/z 525.4 $[M+H]^+$. LC t_R: 1.020 min, purity 95.06%.

4.1.53

3-chloro-4-((4-((1-(4-fluorophenyl)-4-oxo-1,4-dihydro-5H-pyrazolo[3,4-d]pyrimidin-5-yl)methyl)-4-hydroxypiperidin-1-yl)methyl)-N-hydroxybenzamide (**L53**)

Compound **L53** was prepared according to the procedure described for compound **L51**. **L53**: light yellow solid, 31% yield. m.p. 228-230 °C. ^{1}H NMR (300 MHz, d_6-DMSO+D_2O) δ 8.35 (d, *J* = 8.5 Hz, 2H), 8.02 (dd, *J* = 9.0, 4.9 Hz, 2H), 7.85 (d, *J* = 9.3 Hz, 2H), 7.77 (d, *J* = 7.9 Hz, 1H), 7.40 (t, *J* = 8.8 Hz, 2H), 4.41 (s, 2H), 4.08 (s, 2H), 3.18 (d, *J* = 18.4 Hz, 4H), 1.94 (t, *J* = 10.7 Hz, 2H), 1.63 (d, *J* = 14.0 Hz, 2H). ESI-MS: m/z 527.3 $[M+H]^+$. LC t_R: 1.611 min, purity 96.93%.

4.1.54 Methyl 4-((4-((3-bromo-2-methyl-7-oxo-2,7-dihydro-6H-pyrazolo[4,3-d]pyrimidin-6-yl)methyl)-4-hydroxypiperidin-1-yl)methyl)-3-chlorobenzoate (**12**)

Compound **12** was prepared according to the procedure described for compound **L14**. **12**: white solid, 32% yield. m.p. 218-220 °C. ^{1}H NMR (300 MHz, d_6-DMSO) δ 8.03

(s, 1H), 7.98 – 7.84 (m, 2H), 7.65 (d, *J* = 8.4 Hz, 1H), 4.66 (s, 1H), 4.06 (s, 3H), 3.96 (s, 2H), 3.85 (s, 3H), 3.59 (s, 2H), 2.59 – 2.50 (m, 2H), 2.43 – 2.29 (m, 2H), 1.65 – 1.52 (m, 2H), 1.46 – 1.33 (m, 2H). ESI-MS: m/z 524.3 $[M+H]^+$. LC t_R: 0.996 min, purity 98.59%.

4.1.55 Methyl 4-((4-((3-(4-(((tert-butoxycarbonyl)amino)methyl)phenyl)-2-methyl-7-oxo-2,7-dihydro-6H-pyrazolo[4,3-d]pyrimidin-6-yl)methyl)-4-hydroxypiperidin-1-yl)methyl)-3-chlorobenzoate (**17**)

A mixture of **12** (164 mg, 0.31 mmol), **13** (120 mg, 0.36 mmol), $Pd(PPh_3)_4$ (11 mg, 0.0093 mmol) and K_2CO_3 (128 mg, 0.93 mmol) in DMF (3 mL) was degassed under a vacuum and refilled with N_2 three times. The mixture was heated at 110 □ under a N_2 atmosphere for 19 h. After cooling to room temperature, the mixture was partitioned in water (9 mL) and EtOAc (10 mL). The organic layer was collected, and the aqueous layer was extracted with EtOAc (3 x 10 mL). The combined organic layers were dried over Na_2SO_4, concentrated in a vacuum and purified by column chromatography (silica gel, DCM : MeOH = 20 : 1) to give compound **17** (141 mg, 60% yield) as a white solid. m.p. 168-170 °C. ^{1}H NMR (300 MHz, d_6-DMSO) δ 8.00 (s, 1H), 7.98 – 7.85 (m, 2H), 7.76 – 7.59 (m, 3H), 7.54 – 7.35 (m, 3H), 4.67 (s, 1H), 4.22 (d, *J* = 5.9 Hz, 2H), 4.10 (s, 3H), 4.00 (s, 2H), 3.87 (s, 3H), 3.62 (s, 2H), 2.66 – 2.52 (m, 2H), 2.40 (t, *J* = 10.1 Hz, 2H), 1.63 (t, *J* = 10.0 Hz, 2H), 1.42 (s, 11H). ESI-MS: m/z 651.4 $[M+H]^+$. LC t_R: 0.737 min, purity 96.24%.

4.1.56 Methyl 4-((4-((3-(4-(acetamidomethyl)phenyl)-2-methyl-7-oxo-2,7-dihydro-6H-pyrazolo[4,3-d]pyrimidin-6-yl)methyl)-4-hydroxypiperidin-1-yl)methyl)-3-chlorobenzoate (**L54**)

Compound **L54** was prepared according to the procedure described for compound **17**. **L54**: white solid, 65% yield. m.p. 117-119 °C. ^{1}H NMR (300 MHz, d_6-DMSO) δ 8.41 (t, *J* = 5.8 Hz, 1H), 7.99 (s, 1H), 7.89 (d, *J* = 4.8 Hz, 2H), 7.80 – 7.60 (m, 3H), 7.43 (d, *J* = 8.1 Hz, 2H), 4.65 (s, 1H), 4.33 (d, *J* = 5.9 Hz, 2H), 4.08 (s, 3H), 3.98 (s, 2H), 3.85

(s, 3H), 3.60 (s, 2H), 2.63 – 2.52 (m, 2H), 2.45 – 2.32 (m, 2H), 1.89 (s, 3H), 1.73 – 1.55 (m, 2H), 1.51 – 1.34 (m, 2H). ESI-MS: m/z 593.2 $[M+H]^+$. LC t_R: 0.914 min, purity 95.86%.

4.1.57

4-((3-(4-(ammoniomethyl)phenyl)-2-methyl-7-oxo-2,7-dihydro-6H-pyrazolo[4,3-d]pyrimidin-6-yl)methyl)-1-(2-chloro-4-(methoxycarbonyl)benzyl)-4-hydroxypiperidin-1-ium 2,2,2-trifluoroacetate (**L55**)

To a solution of **17** (59 mg, 0.0091 mmol) in DCM (4 mL) was added trifluoroacetic acid (400 µL) at 0 °C. The mixture was stirred for 3 h and concentrated. The residue was suspended in EtOAc (2 mL) and stirred for 4 h at rt. The precipitates were collected by filtration and dried under a vacuum to give compound **L55** (56 mg, 79% yield) as a light yellow solid. m.p. 133-135 °C. ^{1}H NMR (300 MHz, d_6-DMSO) δ 9.69 (s, 1H), 8.34 (s, 3H), 8.12 – 7.94 (m, 3H), 7.92 – 7.82 (m, 1H), 7.77 (d, *J* = 7.6 Hz, 2H), 7.66 (d, *J* = 7.7 Hz, 2H), 5.32 (s, 1H), 4.54 (s, 2H), 4.14 (s, 2H), 4.12 (s, 3H), 4.04 (s, 2H), 3.89 (s, 3H), 2.63 – 2.50 (m, 2H), 1.96 – 1.80 (m, 2H), 1.77 – 1.55 (m, 2H), 1.35 – 1.20 (m, 2H). ^{13}C NMR (75 MHz, d_6-DMSO) δ ppm 165.10, 159.15, 158.68, 156.66, 147.82, 135.35, 134.53, 130.06, 129.70, 118.20, 114.33, 73.51, 68.87, 67.56, 58.24, 56.22, 56.20, 56.17, 53.39, 53.14, 48.61, 42.48, 40.09, 31.92. ESI-MS: m/z 551.3 $[M-2CF_3COOH+H]^+$. LC t_R: 0.941 min, purity 98.11%.

4.2 USP7 enzyme inhibition assay

The inhibitory activity of compounds against USP7 was determined according to a previously described method [30]. Briefly, test compounds were prepared in DMSO with a 1:3 serial dilution starting from 250 µM. Then, the prepared compound solution or vehicle control (DMSO) was added to the reaction buffer (50 mM HEPES, 0.5 mM EDTA, 100 mM NaCl, 1 mM TCEP, 0.1 mg/mL BSA, pH 8.0) containing full-length USP7 (#U-519, Boston Biochem). After incubation for 30 min at room temperature in the dark, the reaction system was initiated by addition of Ub-Rho (Boston Biochem 10 µL, 50 nM) in a white 384-well plate (Thermo Scientific,

264706). The plate was incubated for another 2 h, and the fluorescence intensity (excitation = 485 nm; emission = 535 nm) was measured using an automated microplate spectrophotometer (EnSpire, PerkinElmer). IC_{50} values were calculated by curve fits using GraphPad Prism software.

4.3 X-ray crystallography

The constructs of the USP7 catalytic domains (aa. 208-560 for K_D measurement and aa. 208-554 for X-ray crystallography) in the pET28a vector were expressed in E. coli Rosetta (DE3) cells. The proteins were initially purified by Ni-NTA affinity chromatography and anion exchange chromatography, followed by size exclusion chromatography in PBS buffer containing 0.02% Tween 20 for K_D measurement and in a running buffer of 10 mM Tris-HCl, pH 8.0, 100 mM NaCl, and 4 mM TCEP for X-ray crystallography, respectively.

The X-ray crystallographic study of the USP7 catalytic domain (aa. 208–554) in complex with inhibitors was performed according to the method described by Lorna et al [31]. Briefly, USP7 catalytic domain crystals were grown by hanging-drop vapor diffusion of the protein solution and an equal volume of reservoir solution. Co-crystals of USP7 with compound **L55** were obtained by soaking the above crystals with compound **L55**. The crystals were cryoprotected and flash-frozen in liquid nitrogen for diffraction data collection on the X-ray crystallography facility platform at the National Protein Research Facility (Tsinghua) Base. Data collection and refinement statistics are shown in Table S6 (see Supporting Information).

4.4 K_D Measurement

The affinity of compound binding to the USP7 catalytic domain (aa. 208-560) was examined on an Octet RED96 (FortéBio). Briefly, USP7 was conjugated to biotin in PBS buffer containing 0.02% Tween 20 and immobilized onto Super Streptavidin (SSA) biosensors. Then, three steps were conducted in PBS buffer containing 0.02% Tween 20, 0.1% BSA and 0.4% DMSO: (1) baseline acquisition (600 s), (2) association (120 s) for the measurement of K_a, and (3) dissociation (180 s) for K_D

measurement. All the steps were performed at 30 °C. At least four concentrations of compounds were used for detection. The association and dissociation plots and kinetic constants (K_a, K_d, and K_D) were obtained with FortéBio data analysis software.

4.5 Cell viability assay

Tumor cells were seeded at an appropriate density (LNCaP, 2500 cells/well; RS4;11, 5000 cells/well; HCT-116, Huh7, K562 and NB4, 2000 cells/well) into 96-well plates. After 24 h, the cells were treated with different concentrations of compounds for specific times (LNCaP, 6 days; RS4;11, HCT-116, Huh7, K562 and NB4, 3 days). Cell viability was determined using the CellTiter-Glo assay with an automated microplate spectrophotometer (EnSpire, PerkinElmer). IC_{50} values were calculated with GraphPad Prism version 5.0.

Declaration of competing interest

The authors declare no competing financial interests.

Acknowledgments

Financial support from the National Natural Science Foundation of China (91853125, 81773584 and 21977118) is gratefully acknowledged. This research was also supported by the Jiangsu Provincial Key Research and Development Program (BE2018710), the National Science & Technology Major Project “Key New Drug Creation and Manufacturing Program”, China (2019ZX09201001-003-004 and 2019ZX09301-151), the “Double First-Class” University Project (CPU2018GY45) and the BAGUI Scholar Program of Guangxi Province of China (2016A13). Dr. Shilong Fan from Beijing Advanced Innovation Center for Structural Biology at Tsinghua University provided technical assistance for the X-ray crystallographic study.

Supporting Information

References

1. Kwon, Y. T.; Ciechanover, A. The ubiquitin code in the ubiquitin-proteasome system and autophagy. *Trends Biochem Sci* **2017,** 42, 873-886.
2. Hershko, A.; Ciechanover, A. The ubiquitin system. *Annu Rev Biochem* **1998,** 67, 425-479.
3. Pinto-Fernandez, A.; Kessler, B. M. DUBbing cancer: deubiquitylating enzymes involved in epigenetics, DNA damage and the cell cycle as therapeutic targets. *Front Genet* **2016,** 7.
4. Maculins, T.; Fiskin, E.; Bhogaraju, S.; Dikic, I. Bacteria-host relationship: ubiquitin ligases as weapons of invasion. *Cell Res* **2016,** 26, 499-510.
5. Ciechanover, A.; Kwon, Y. T. Degradation of misfolded proteins in neurodegenerative diseases: therapeutic targets and strategies. *Exp Mol Med* **2015,** 47, e147.
6. Chen, D.; Frezza, M.; Schmitt, S.; Kanwar, J.; Dou, Q. P. Bortezomib as the first proteasome inhibitor anticancer drug: current status and future perspectives. *Curr Cancer Drug Tar* **2011,** 11, 239-253.
7. Leznicki, P.; Kulathu, Y. Mechanisms of regulation and diversification of deubiquitylating enzyme function. *J Cell Sci* **2017,** 130, 1997-2006.
8. Harrigan, J. A.; Jacq, X.; Martin, N. M.; Jackson, S. P. Deubiquitylating enzymes and drug discovery: emerging opportunities. *Nat Rev Drug Discov* **2018,** 17, 57-77.
9. Haq, S.; Suresh, B.; Ramakrishna, S. Deubiquitylating enzymes as cancer stem cell therapeutics. *BBA-Rev Cancer* **2018,** 1869, 1-10.
10. Tian, Z.; D'Arcy, P.; Wang, X.; Ray, A.; Tai, Y. T.; Hu, Y. G.; Carrasco, R. D.; Richardson, P.; Linder, S.; Chauhan, D.; Anderson, K. C. A novel small molecule inhibitor of deubiquitylating enzyme USP14 and UCHL5 induces apoptosis in multiple myeloma and overcomes bortezomib resistance. *Blood* **2014,** 123, 706-716.
11. Li, M. Y.; Chen, D. L.; Shiloh, A.; Luo, J. Y.; Nikolaev, A. Y.; Qin, J.; Gu, W. Deubiquitination of p53 by HAUSP is an important pathway for p53 stabilization. *Nature* **2002,** 416, 648-653.
12. Li, M. Y.; Brooks, C. L.; Kon, N.; Gu, W. A dynamic role of HAUSP in the p53-Mdm2 pathway. *Mol Cell* **2004,** 13, 879-886.
13. Cummins, J. M.; Rago, C.; Kohli, M.; Kinzler, K. W.; Lengauer, C.; Vogelstein, B. Disruption of HAUSP gene stabilizes p53. *Nature* **2004,** 428.
14. Cummins, J. M.; Vogelstein, B. HAUSP is required for p53 destabilization. *Cell Cycle* **2004,** 3, 689-692.
15. van Loosdregt, J.; Fleskens, V.; Fu, J.; Brenkman, A. B.; Bekker, C. P. J.; Pals, C. E. G. M.; Meerding, J.; Berkers, C. R.; Barbi, J.; Grone, A.; Sijts, A. J. A. M.; Maurice, M. M.; Kalkhoven, E.; Prakken, B. J.; Ovaa, H.; Pan, F.; Zaiss, D. M. W.; Coffer, P. J. Stabilization of the transcription factor Foxp3 by the deubiquitinase USP7 increases Treg-cell-suppressive capacity. *Immunity* **2013,** 39, 259-271.
16. Tavana, O.; Li, D.; Dai, C.; Lopez, G.; Banerjee, D.; Kon, N.; Chen, C.; Califano, A.; Yamashiro, D. J.; Sun, H.; Gu, W. HAUSP deubiquitinates and stabilizes N-Myc in neuroblastoma. *Nat Med* **2016,** 22, 1180-1186.
17. Wang, L. Q.; Kumar, S.; Dahiya, S.; Wang, F.; Wu, J.; Newick, K.; Han, R. X.; Samanta, A.; Beier, U. H.; Akimova, T.; Bhatti, T. R.; Nicholson, B.; Kodrasov, M. P.;

Agarwal, S.; Sterner, D. E.; Gue, W.; Weinstock, J.; Butt, T. R.; Albelda, S. M.; Hancock, W. W. Ubiquitin-specific protease-7 inhibition impairs Tip60-dependent Foxp3+ T-regulatory cell function and promotes antitumor immunity. *Ebiomedicine* **2016,** 13, 99-112.

18. Wang, F.; Wang, L.; Wu, J.; Sokirniy, I.; Nguyen, P.; Bregnard, T.; Weinstock, J.; Mattern, M.; Bezsonova, I.; Hancock, W. W.; Kumar, S. Active site-targeted covalent irreversible inhibitors of USP7 impair the functions of Foxp3+ T-regulatory cells by promoting ubiquitination of Tip60. *PLoS One* **2017,** 12, e0189744.

19. Nicholson, B.; Kumar, K. G. S. The multifaceted roles of USP7: new therapeutic opportunities. *Cell Biochem Biophys* **2011,** 60, 61-68.

20. Colland, F.; Formstecher, E.; Jacq, X.; Reverdy, C.; Planquette, C.; Conrath, S.; Trouplin, V.; Bianchi, J.; Aushev, V. N.; Camonis, J.; Calabrese, A.; Borg-Capra, C.; Sippl, W.; Collura, V.; Boissy, G.; Rain, J. C.; Guedat, P.; Delansorne, R.; Daviet, L. Small-molecule inhibitor of USP7/HAUSP ubiquitin protease stabilizes and activates p53 in cells. *Mol Cancer Ther* **2009,** 8, 2286-95.

21. Reverdy, C.; Conrath, S.; Lopez, R.; Planquette, C.; Atmanene, C.; Collura, V.; Harpon, J.; Battaglia, V.; Vivat, V.; Sippl, W.; Colland, F. Discovery of specific inhibitors of human USP7/HAUSP deubiquitinating enzyme. *Chem Biol* **2012,** 19, 467-77.

22. Chauhan, D.; Tian, Z.; Nicholson, B.; Kumar, K. G. S.; Zhou, B.; Carrasco, R.; McDermott, J. L.; Leach, C. A.; Fulcinniti, M.; Kodrasov, M. P.; Weinstock, J.; Kingsbury, W. D.; Hideshima, T.; Shah, P. K.; Minvielle, S.; Altun, M.; Kessler, B. M.; Orlowski, R.; Richardson, P.; Munshi, N.; Anderson, K. C. A small molecule inhibitor of ubiquitin-specific protease-7 induces apoptosis in multiple myeloma cells and overcomes bortezomib resistance. *Cancer Cell* **2012,** 22, 345-358.

23. Turnbull, A. P.; Ioannidis, S.; Krajewski, W. W.; Pinto-Fernandez, A.; Heride, C.; Martin, A. C. L.; Tonkin, L. M.; Townsend, E. C.; Buker, S. M.; Lancia, D. R.; Caravella, J. A.; Toms, A. V.; Charlton, T. M.; Lahdenranta, J.; Wilker, E.; Follows, B. C.; Evans, N. J.; Stead, L.; Alli, C.; Zarayskiy, V. V.; Talbot, A. C.; Buckmelter, A. J.; Wang, M.; McKinnon, C. L.; Saab, F.; McGouran, J. F.; Century, H.; Gersch, M.; Pittman, M. S.; Marshall, C. G.; Raynham, T. M.; Simcox, M.; Stewart, L. M. D.; McLoughlin, S. B.; Escobedo, J. A.; Bair, K. W.; Dinsmore, C. J.; Hammonds, T. R.; Kim, S.; Urbe, S.; Clague, M. J.; Kessler, B. M.; Komander, D. Molecular basis of USP7 inhibition by selective small-molecule inhibitors. *Nature* **2017,** 550, 481-486.

24. Gavory, G.; O'Dowd, C. R.; Helm, M. D.; Flasz, J.; Arkoudis, E.; Dossang, A.; Hughes, C.; Cassidy, E.; McClelland, K.; Odrzywol, E.; Page, N.; Barker, O.; Miel, H.; Harrison, T. Discovery and characterization of highly potent and selective allosteric USP7 inhibitors. *Nat Chem Biol* **2018,** 14, 118-125.

25. O'Dowd, C. R.; Helm, M. D.; Rountree, J. S. S.; Flasz, J. T.; Arkoudis, E.; Miel, H.; Hewitt, P. R.; Jordan, L.; Barker, O.; Hughes, C.; Rozycka, E.; Cassidy, E.; McClelland, K.; Odrzywol, E.; Page, N.; Feutren-Burton, S.; Dvorkin, S.; Gavory, G.; Harrison, T. Identification and structure-guided development of pyrimidinone based USP7 inhibitors. *ACS Med Chem Lett* **2018,** 9, 238-243.

26. Lamberto, I.; Liu, X.; Seo, H. S.; Schauer, N. J.; Iacob, R. E.; Hu, W.; Das, D.;

Mikhailova, T.; Weisberg, E. L.; Engen, J. R.; Anderson, K. C.; Chauhan, D.; Dhe-Paganon, S.; Buhrlage, S. J. Structure-guided development of a potent and selective non-covalent active-site inhibitor of USP7. *Cell Chem Biol* **2017,** 24, 1490-1500 e11.

27. Fan, J.; Ye, Y.; Chu, G.; Zhang, Z.; Fu, Y.; Li, Y. M.; Shi, J. Semisynthesis of ubiquitin and SUMO-rhodamine 110-glycine through aminolysis of Boc-protected thioester counterparts. *J Org Chem* **2019,** 84, 14861-14867.

28. Tan, X. D.; Bai, J. S.; Ding, S.; Ren, Y. J.; Hong, D. N.; Mei, Z. Q.; Li, Y. M. Semi-synthesis of ubiquitin-propargylamide for identifying deubiquitinase targeting inhibitors. *Chinese Chem Lett* **2019,** 30, 743-746.

29. Zhou, J.; Wang, J. Z.; Chen, C.; Yuan, H. L.; Wen, X. A.; Sun, H. B. USP7: target validation and drug discovery for cancer therapy. *Med. Chem.* **2018,** 14, 3-18.

30. Chen, C.; Song, J.; Wang, J.; Xu, C.; Chen, C.; Gu, W.; Sun, H.; Wen, X. Synthesis and biological evaluation of thiazole derivatives as novel USP7 inhibitors. *Bioorg Med Chem Lett* **2017,** 27, 845-849.

31. Kategaya, L.; Di Lello, P.; Rouge, L.; Pastor, R.; Clark, K. R.; Drummond, J.; Kleinheinz, T.; Lin, E.; Upton, J. P.; Prakash, S.; Heideker, J.; McCleland, M.; Ritorto, M. S.; Alessi, D. R.; Trost, M.; Bainbridge, T. W.; Kwok, M. C. M.; Ma, T. P.; Stiffler, Z.; Brasher, B.; Tang, Y.; Jaishankar, P.; Hearn, B. R.; Renslo, A. R.; Arkin, M. R.; Cohen, F.; Yu, K.; Peale, F.; Gnad, F.; Chang, M. T.; Klijn, C.; Blackwood, E.; Martin, S. E.; Forrest, W. F.; Ernst, J. A.; Ndubaku, C.; Wang, X.; Beresini, M. H.; Tsui, V.; Schwerdtfeger, C.; Blake, R. A.; Murray, J.; Maurer, T.; Wertz, I. E. USP7 small-molecule inhibitors interfere with ubiquitin binding. *Nature* **2017,** 550, 534-538.

Highlights

- Fifty-five piperidinol derivatives were synthesized and biologically evaluated.
- Compound **L55** exhibited potent USP7 inhibitory activity (IC_{50} = 40.8 nM).
- X-ray crystallographic studies revealed a new pose for **L55** to bind to USP7.
- **L55** downregulated MDM2 and DNMT1 and upregulated p53 and p21 in RS4;11 cells.
- LNCaP (IC_{50} = 29.6 nM) and RS4;11 (IC_{50} = 41.6 nM) were highly sensitive to **L55**.

Declaration of interests

☒ The authors declare that they have no known competing financial interests or personal relationships that could have appeared to influence the work reported in this paper.

☐The authors declare the following financial interests/personal relationships which may be considered as potential competing interests: